THE IMPACT OF STORM ON THERMAL TRANSPORT IN THE HYPORHEIC ZONE OF A LOW-GRADIENT THIRD-ORDER SAND AND GRAVEL BEDDED STREAM

Erasmus K. Oware

74 Pages August 2010

This study assesses the impact of storms on thermal transport within the hyporheic zone of a low gradient sand and gravel bedded stream in central Illinois.

APPROVED:

_____

Date Eric Peterson, Chair

_____

Date Stephen Van der Hoven

_____

Date Dagmar Budikova

THE IMPACT OF STORM ON THERMAL TRANSPORT IN THE HYPORHEIC ZONE OF A LOW GRADIENT THIRD-ORDER SAND AND GRAVEL BEDDED STREAM

Erasmus K. Oware

74 Pages August 2010

The importance of temperature in stream and hyporheic exchange and its impact on lotic systems are far reaching, and one event that affects temperature in the hyporheic zone (HZ) is a storm (high flow) event. The goal of this study was to evaluate the impacts of storm events on thermal transport in the HZ of low gradient sand and gravel bedded stream. Six (6) wells were installed along a 25 m straight stretch along the Little Kickapoo Creek (LKC) at Mclean County, Illinois, USA. Analysis of the HZ temperature profiles revealed a clear seasonal thermal reverse in the After-Storm Substrate Temperature Change (ASSTC), which was due the direction of the pre-storm thermal gradient between the stream and substrate temperatures. Advective transport dominates heat transfer in the upper substrate, whereas, conductive transport dominates heat transmission into the deeper substrate depending on the depth of wetting front of the storm. The overall Peclet number (P_e) = 34.1 is an indication of overall dominance of

advection in the vertical transmission of ASSTC. The results further indicated a decay in the amplitude of the vertical responses with increasing depth. The p-values of t-test of equality of means, however, showed no significant differences in the dampening responses with increasing depth up to the 150 cm depth in the summer, whereas, the winter response showed significant difference at 150 cm depth at 0.05 significant level. A predictive model based on the amplitude of storm and pre-storm stream temperature was fitted to simulate ASSTC. The overall findings of this research highlight the need to incorporate storm events in the numerous studies of hyporheic heat transport. It will also aid resource managers in the investigation and management of aquatic ecosystems notably within the HZ.

APPROVED:

_____

Date Eric Peterson, Chair

_____

Date Stephen Van der Hoven

_____

Date Dagmar Budikova

THE IMPACT OF STORM ON THERMAL TRANSPORT IN THE HYPORHEIC ZONE OF A LOW-GRADIENT THIRD-ORDER SAND AND GRAVEL BEDDED STREAM

ERASMUS K. OWARE

A Thesis Submitted in Partial
Fulfillment of the Requirements
for the Degree of

MASTER OF SCIENCE

Department of Geography-Geology

ILLINOIS STATE UNIVERSITY

2010

THE IMPACT OF STORM ON THERMAL TRANSPORT IN THE HYPORHEIC ZONE OF A LOW-GRADIENT THIRD-ORDER SAND AND GRAVEL BEDDED STREAM

ERASMUS K. OWARE

THESIS APPROVED:

Date	Eric Peterson, Chair
Date	Stephen Van der Hoven
Date	Dagmar Budikova

AKNOWLEDGEMENTS

I would first and foremost express my sincere gratitude to my thesis adviser Dr. Eric Peterson, for his constructive criticism that has honed my writing ability. This project would not have been possible without his input. I would also like to thank my other thesis committee members, Dr. Stephen Van der Hoven for his guidance and his always availability to assist and advise me, and Dr. Dagmar Budikova for the geostatistics class which forms the basis of this project. The geostatistics class has given me a new dimension in approaching data analysis. I would further like to thank the faculty of the Department of Geography-Geology, for their support and encouragement through the years, which made my stay in the cold Illinois weather a possibility. I would also like to give a huge thanks to all my friends, who assisted me in one way or the other throughout the past 2 years. Hridaya, thanks for all the support in installing the wells in the cold stream. Lastly, I would like to thank my family back in Ghana for their patience and encouragement, it has not been easy without you but it was for sure for a good purpose. Can't wait to reunite with you.

E. K. O.

CONTENTS

TABLE

FIGURE

CHAPTER I

GENERAL INTRODUCTION

Introduction

Background

Dr. T. C. Winter is the vanguard in the field of groundwater and surface water interaction. He studied a series of field and numerical analyses demonstrating the conditions under which groundwater components can be significant contributors to surface water budget (Winter, 1978a, b, 1981, 1983, 1986). Groundwater and surface water interaction has since gained increasing attention with several authors using different techniques to demonstrate groundwater and surface water interactions. In order to characterize groundwater system to identify areas of groundwater inflows, Winter (1986) and Keneoyer and Anderson (1989) used extensive arrays of boreholes and/or piezometers to monitor groundwater inflows to lakes.

Due to cost and cumbersomeness of using arrays of boreholes, several authors have tried to find alternative cheap and less cumbersome techniques in studying groundwater and surface water interaction. Cartwright *et al.* (1979) measured pressure gradient within sediments in deep lakes using a probe consisting of multiple pressure transducers. Lee (1977) determined rate of groundwater inflow (outflow) to lakes using seepage meters. Atwel et al. (1971), Souto-Maior (1973) and Nelson (1991) used thermal remote sensing to delineate locations of influence of natural and forced inflows to surface water bodies. Lee (1985), furthermore, used thermal and electrical-conductivity signatures in the lake and sediments to identify groundwater inflows to the lake. Consequently, Silliman and Booth (1992), extended the work of Nelson (1991) and the sediment monitoring of Lee (1985), combined with sediment temperatures as indicator of diffuse groundwater inflow to a creek. The work of Silliman and Booth (1993) opened a new paradigm in the use of sediment temperature in the study of groundwater and surface water interactions.

The hyporheic zone (HZ) (Figure I-1) is defined as the interface below the streambed where groundwater and surface water mix (Conant, 2004; Hayashi and Rosenberry, 2002) or where surface water infiltrates into biologically active near stream sediments. (Boulton *et al.,* 1998). The groundwater and stream interaction links the geochemistry, biology, and hydrology of the stream with the substrate (Bencala, 2000).

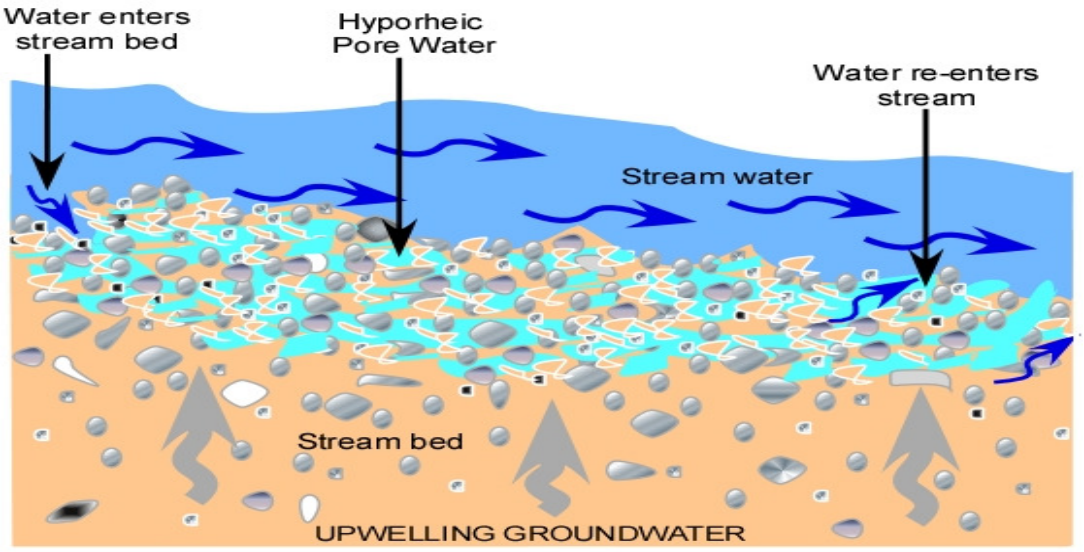

Figure I-1: Schematic illustration of the hyporheic zone below a stream.

The development of various research techniques has made temperature a very important tool in HZ studies. Since heat is an important nonreactive, naturally occurring, robust tracer (Constantz et al., 2003), the new techniques based on heat as a tracer have led to a cost-effective and accurate method of analyzing groundwater-stream interactions (Anderson, 2005; Stonestrom and Constantz, 2004).

Approach

HZ study is traditionally interdisciplinary due to interaction of geomorphological, hydrological, and ecological processes. Subsequently, one event that will affect heat in the HZ is a storm-induced high hydrological flow and to some extent the gradient of the stream. Due to interdisciplinary nature of HZ studies, the objectives and research questions of this paper were proposed with aquatic and ecological studies in mind. The results will help in the investigation and management of biotic and abiotic interactions.

Project Overview

There have been numerous research works on temperature transmission in stream and in HZ and numerous attempts to build predictive models to simulate stream temperatures. Kobayashi et al. (1999) and Brown and Hannah (2007) hypothesized that precipitation may cause changes in stream temperature due to direct inputs and by inducing runoff from/via various hydrological stores/pathways. Since high hydrologic flow will increase seepage into the streambed, the changes in stream temperature due to the precipitation will thus, be transmitted into the streambed. Additionally, the geomorphology of a stream also affects the residence time and seepage into the streambed. However, the area of research of the impact of storm induced high hydrologic flow on HZ temperature transmission and research in fitting a predictive model to simulate after-storm HZ temperatures of a low-gradient sand and gravel bedded stream remain completely unexploited. The focus of this paper is to help bridge this research gap through two main approaches: (1) thermal variations approach and, (2) predictive model approach.

Chapter 2 of this research work was designed to evaluate how seasonal changes affect after-storm thermal variations in the substrate and to quantify the thermal variations with increasing substrate depth. Additionally, **Chapter 3** was set up to assess the main factors or parameters that control the substrate after-storm thermal response for the various seasons and to fit a predictive model to simulate the ASSTC using the resulting main controlling parameters. Finally, **Chapter 4** summarizes the results from both approaches.

CHAPTER II

THERMAL VARIATIONS APPROACH

Abstract

The importance of temperature in stream and hyporheic exchange is far reaching, and one event that affects temperature in the hyporheic zone (HZ) is a storm (high flow) event. The goal of this study was to evaluate the impacts of storm events on thermal transport in the HZ of a low gradient sand and gravel bedded stream. Six (6) wells were installed along a 25 m straight stretch along the Little Kickapoo Creek (LKC) at Mclean County, Illinois, USA. Analysis of the HZ temperature profiles revealed a clear seasonal thermal reverse in the After-Storm Substrate Temperature Change (ASSTC). There were spikes in the ASSTC in the summer and drops in the winter, which was due the direction of the pre-storm thermal gradient between the stream and substrate temperatures. Advective transport dominates heat transfer in the upper substrate, whereas, conductive transport dominates heat transmission into the deeper substrate depending on the depth of wetting front of the storm. The overall Peclet number (P_e) = 34.1 is an indication of overall dominance of advection in the vertical transmission of ASSTC. In addition to advection and conduction controlling vertical temperature transmission into the substrate, the amplitude of the vertical responses decayed with increasing depth. The p-values of t-test of equality of means, however, showed no significant differences in the dampening responses with increasing depth up to the 150 cm depth in the summer, whereas, the winter response showed significant difference at 150 cm depth at 0.05 significant level. The overall findings of this research highlight the need to incorporate storm events in the numerous studies of hyporheic heat transport.

Introduction

Heat is an important nonreactive naturally occurring robust tracer (Constantz et al., 2003) that can be used to indentify water movement, quantify groundwater fluxes and aquifer hydraulic properties, and to delineate losing and gaining reaches of a stream (Bouyoucos, 1915; Suzuki, 1960; Lee, 1985; Lapham, 1989; Silliman and Booth 1993). Major external drivers that determine how much heat is added or taken from a river thermal system are direct and indirect solar radiation, air temperature, groundwater inputs, and wind speed (Sullican and Adams, 1991). The development of various research techniques has made temperature a very important tool in the study of groundwater-stream interaction. These new techniques in using heat as a tracer have led to a cost-effective and accurate method of analyzing groundwater-stream interactions (Anderson, 2005; Stonestrom and Constantz, 2004).

The hyporheic zone (HZ) is defined as the interface below the streambed where groundwater and surface water mix or where surface water infiltrates into biologically active near stream sediments. (Boulton *et al.,* 1998; Conant, 2004; Hayashi and Rosenberry, 2002). The evaluation of streambed temperature profiles can be used to quantify groundwater-stream interactions (Stonestrom and Constantz, 2003), delineate flow paths in the (HZ) (Conant, 2004), and assist in the evaluation of factors that generate change within thermal profiles (Malard, et al., 2001). The streambed has been identified as a potentially important heat source/sink affecting the overlying water channel (Evans *et al.* 1998; Hannah *et al.* 2004) with streambed temperature profile reflecting the nature and extent of groundwater-surface water interactions (Malcolm *et al.* 2004; Brown *et al.* 2005).

The HZ is ecologically significant as a hatchery for salmonid and invertebrate eggs (Hynes, 1983; Shepherd, 1984), as a refuge for invertebrates and larval fish during spates (high flows) (Hynes *et al,* 1976; Poole & Stewart, 1976), and an important zone for stream metabolism (Grimm & Fisher, 1984; Valett *et al.,* 1990). The HZ also may provide a refuge from thermal fluctuations induced by seasonal changes, frontal passages, diurnal variations, and anthropogenic impacts (Brunke and Gosner 1997; Dole-Olivier and Marmonier 1992; Dole-Olivier et al. 1997; Grimm *et al*. 1991; Stanford and Ward 1993; Williams 1984). Thus, if the HZ provides refuge to invertebrate and fish during spates and provides refuge from thermal fluctuations, then the importance of thermal transport to aquatic stability within the hyporheic zone during spates cannot be overemphasized. Studies have shown that the magnitude of river flow affects significantly the chemical, physical and biological gradients within the HZ which in effect affects the structure and function of aquatic ecosystems (Stanford and Ward, 1993; Curry et al., 1994; Fraser et al., 1996; Wroblicky et al., 1998; Soulsby *et al*., 2001) and HZ water quality (Arntzen *et al*., 2006). There is an acute change in HZ and stream temperatures during storm events. Galloway and Kieffer (2003) showed that acute decrease and acute increase in temperature affect osmotic balance of salmon. While salmon recovery was enhanced by acute increase in temperature, an acute decrease in temperature slows the recovery of various muscle and blood metabolites.

Additionally, temperature is a basic parameter that controls physical, ecological and biogeochemical activities in aquatic systems and controls habitat diversity (Hynes, 1970; Ward, 1985; Poole and Berman, 2001). Periphyton metabolism is dependent on water flux under isothermal conditions (Hondzo and Wang, 2002) and recent studies have

shown the sensitiveness of temperature on periphyton productivity (e.g. Morin *et al.,* 1999; Karlsson *et al.,* 2005; Kishi *et al.,* 2005). Ecological processes such as organic matter decomposition, fish egg incubation, and invertebrate diapauses are controlled by the thermal regime of the HZ (Silliman *et al,* 1995; Hondzo & Stefan, 1994).

In the recent past, surface water and groundwater were regarded as distinct resources that could be used and studied separately. However, studies have shown that groundwater and surface water systems are hydraulically connected and that the sustained depletions of one resource negatively impacts the other (Glennon, 2002; Baskaran, 2009). Analysis of temperature profiles within the HZ could be used to explain different processes in hyporheic-stream exchange. For instance, Silliman and Booth (1993) demonstrated the use of HZ temperature profiles to delineate losing and gaining portions of a stream in Indiana using the method of diffuse inflow. This knowledge of gaining and losing reaches of a stream could be used to identify biological and biogeochemical hot spots in a stream. There is biological abundance and diversity in groundwater discharge reaches (Hedin *et al*., 1998; Hunt et al., 2006). Additionally, HZ temperature could be used to estimate the degree and duration of percolation of surface water into the streambed. The transfer of diurnal stream temperature pulse into the streambed is an indication of vertical movement rate of water to or from the stream (Conant, 2004; Lampham, 1989). Constantz and Thomas (1996) did a stellar job in demonstrating how streambed temperature profiles could be used as indicators of percolation of stream water into the streambed and Keery *et al.* (2007) used the lag time in conjunction with the rate of change in the amplitude of diurnal temperature signal with depth to estimate the seepage rate.

Consequently, if temperature plays such an important role in groundwater and surface water interactions and in ecologic stability, then factors affecting temperature, and hence the HZ, must be of importance to all these research works. One major factor that affects HZ temperature is hydrological storm (elevated flow) events. The purpose of this work is to study the impacts of high flow events on thermal variations within the HZ of sand and gravel bedded stream. Similar studies have been done in other environments; thermal variations due to storm-induced events in the HZ of karst (White *et al*., 1987; Dogwiler and Wicks, 2006) and alpine (Brown and Hannah, 2006) streams. Dogwiler and Wicks (2006) in their studies in a karst stream saw an after-storm temperature spike of 0-5^{o}C in the substrate, which decreased with increasing depth during the summer, and the magnitude of the temperature spike strongly correlated with the magnitude of the precipitation. They discovered dramatic drop in after-storm substrate temperature during the winter, which was due to the influx of very cold water into the substrate system. Furthermore, the work of Brown and Hannah (2006) in an alpine stream during summer (2002 and 2003), revealed a spatial and temporal differences in after-storm water and substrate thermal responses. There were temperature drops of up to 10.4^{o}C and spikes of 2.3^{o}C in stream water, and a negative relationship between the magnitude of a storm and the after-storm temperature depressions. They also revealed dampening after-storm substrate response with increasing depth. However, none is known of storm-induced events on thermal variations in the HZ of low gradient sand and gravel bedded streams.

This research is focused on evaluating the impact of storm events on thermal transport in the HZ of low gradient sand and gravel bedded stream. Knowledge of thermal transmission in the HZ during storm events will help resource managers in

assessing the impact of acute HZ temperature changes on fish egg incubation, on invertebrate diapauses, and on osmotic balance of fishes. Studies of thermal transmission within the HZ during storm events will also help resource managers to estimate the rate (quantity) of water lost in a stream in order to factor the quantity of water lost in their water budget. The insight to this objective is provided by exploring the following research questions:

1. What is the seasonal behavior of after storm substrate thermal response?
2. How does after storm substrate thermal response vary with increasing substrate depth?

Methodology

Study Locality

A 25 m straight stretch along the Little Kickapoo Creek (LKC) located in Mclean County in Central Illinois, USA, was selected for the purposes of this investigation (Figure II-1). The LKC is a low gradient third-order perennial gaining stream with a general gradient of 0.002 (Peterson and Sickbert, 2006).

Three geologic units make up the alluvial valley along the stretch of the study site (Figure II-1). These include the Wedron Formation (WF), the Henry Formation (HF), and the Cahokia Formation (CF), listed from oldest to youngest. The WF acts as a lower confining unit to the HF, being a clay-rich low-permeable till with some interstitial sand and gravel deposited by past glacial activity.

The stream cuts through the CF and the channel runs through the HF. The main aquifer is the HF because of its moderately sorted gravels and sands, with an average hydraulic conductivity of 10m/day and an average thickness of 5-7 m in the outwash valley. The CF lies above the HF and it is made up of silt and clay, with some interstitial sand lenses. Repeated flooding of LKC formed the CF with an average thickness of approximately 2 meters across the outwash valley. The CF is not considered a confining unit because of the presence of macro porosity and high level of connectivity between LKC and HF.

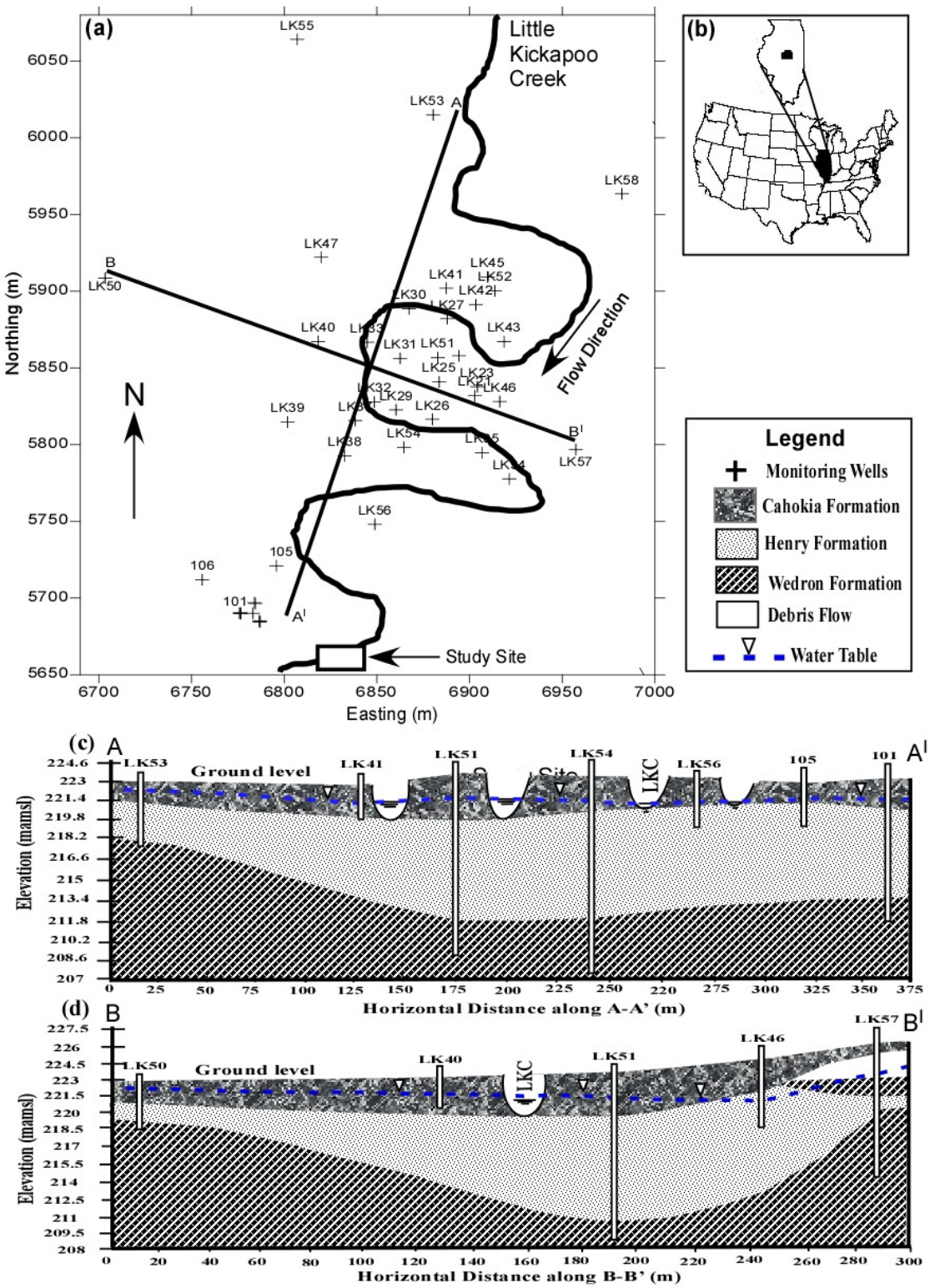

Figure II-1: a) Figure showing an aerial map of the Randolph well field study area with cross section line locations, b) the US state map showing Illinois State and McLean County, c and d) Cross sections along lines A-A^{l} and B-B^{l} respectively.

Climatic Setting

Central Illinois has a humid continental climate with cold winters and warm summers. Between the periods of 1950 to 2002, the annual mean temperature was 11.2°C (Peterson and Sickbert, 2006). Specifically, Bloomington, IL climate is warm during summer when temperatures tend to be in the 20 - 30^{o}C range and cold during winter when temperatures are between –1 to –10^{o}C. July is the warmest month of the year with an average maximum temperature of 30^{o}C, while January is the coldest month with an average minimum temperature of –10^{o}C. There are moderate temperature variations between night and day during the summer with a variation of about ± 6.1^{o}C, and an increase variation between night and day temperatures during winter with an average difference of ±7.8^{o}C. The total annual precipitation at Bloomington is 952.75 mm with the wet season in spring and the dry season in winter (Table II-1). All the data are available at the Bloomington Waterworks Weather Station, which is about ten miles upstream of the study site. Ants damaged the weather station set up at the study site.

Table II-1: Annual precipitation of Bloomington

Month	Jan	Feb	Mar	April	May	June	July	Aug	Sep	Oct	Nov	Dec	Annual
Millimeters	36.6	42.4	76.5	90.9	108.5	101.4	95.8	93.0	84.6	66.3	81.5	73.4	952.8

Data Collection

A well grid was set up at the selected study site along riffles within the LKC using a drive-point installation method. The site consisted of six wells (W1, W2, W3, W4, W5 and W6) creating longitudinal profile lines along the stream channel (Figure II-2). Temperature loggers were positioned at multiple depths of 30 cm, 60 cm, 90 cm, and 150

cm within each 6.35 cm PVC well (Figure II-3). Each chamber was separated using foam sealant to prevent vertical mixing of the water in the well.

Separate temperature loggers were attached to W1 and W6 to record upstream and downstream surface water temperatures respectively. A stilling well was located at the bank of the stream in line with well 2 to record the stream stage (Figure II-2). All loggers were programmed to record temperatures at 15-minute intervals due to time needed for the loggers to respond to changes in temperature within the system. Data were collected from February 2009 until March 2010. A total of 41 storms were recorded during this period, making up of 24 storms during the summer period (later spring to early autumn) and 17 storms during the winter period (later autumn to early spring).

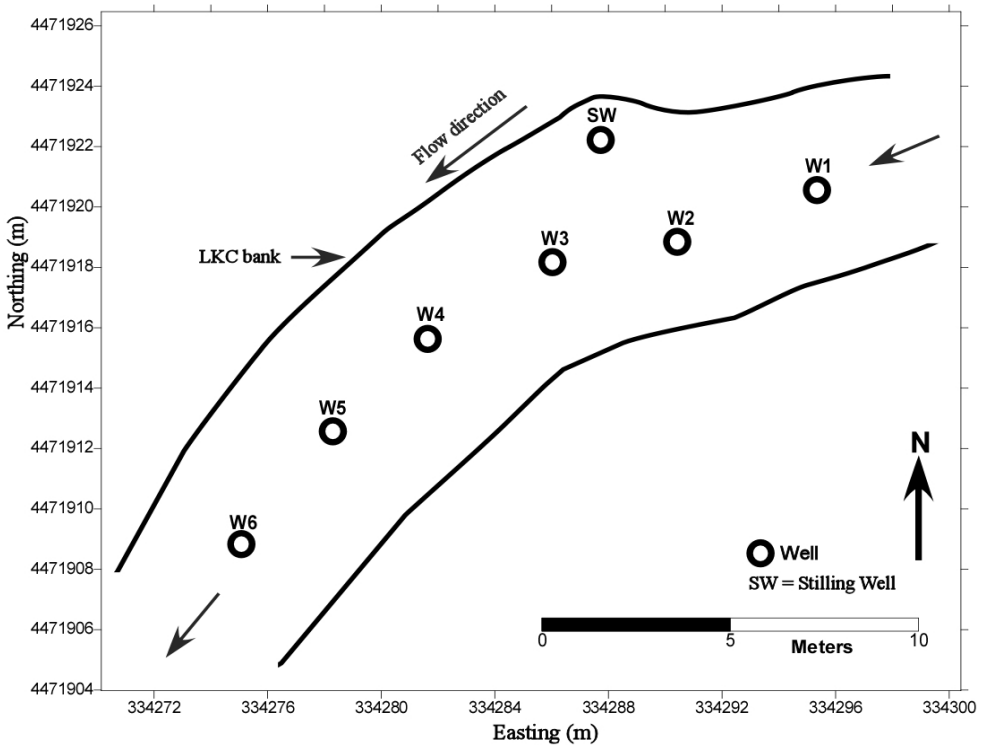

Figure II-2: Birds-eye view of well setup in the stream channel. The numbers indicate respective well names used.

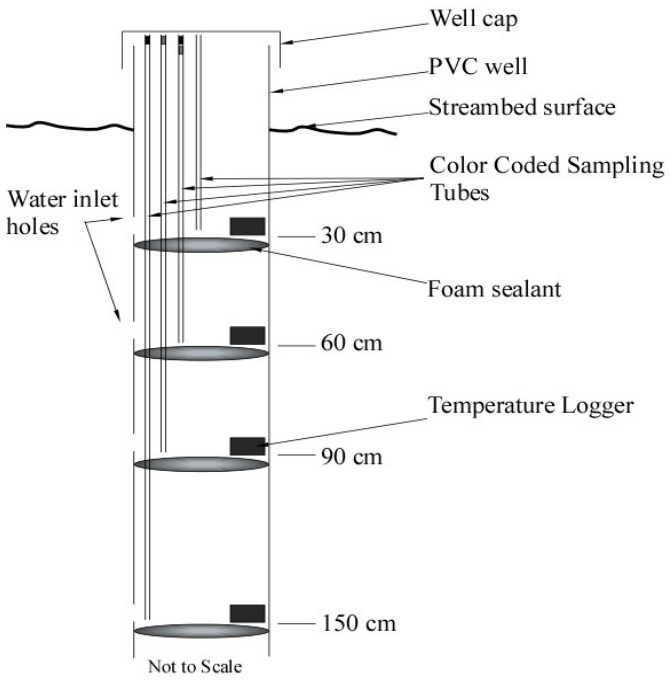

Figure II-3: Detailed view of individual well design

Data Reduction

A hydrograph of the stream stage data was plotted to identify periods of high flow and to extract the storm events. The extracted storm events were compared with precipitation data collected from the US weather service for Bloomington in order to separate storm events from diurnal rises. The amplitude of storm was calculated by subtracting the pre-storm (baseflow) stream stage from the peak-storm stream stage. Thermographs for all loggers in all wells at the various depths and the stream were also plotted and compared to the hydrographs to locate the streambed and stream thermal responses as a result of the storm pulse coming through. The amplitudes of the streambed and stream thermal pulses due to the storm pulse were extracted by subtracting the pre-storm temperature from the peak-storm temperature to get the After-Storm Substrate

Temperature Change (ASSTC). The average of all the ASSTC for each depth in all wells was calculated to represent the ASSTC for a particular storm for that depth. This was done to avoid redundancy of data and to get rid of noise in the data.

Methods of Temperature Comparisons

To study the seasonal variations, the averages of the ASSTC for each depth from all the storms were separated into summer period (later spring to early autumn) data and winter period (later autumn to early spring) data. A summary of the total number of average ASSTC of each storm at all depths is provided in Table II-2. Histograms and box plots were plotted for the substrate temperature changes for the two seasons to compare whether the data from the two seasons belong to the same distribution or not. Descriptive statistics and box plots of the pre and peak-storm of the stream temperatures and the substrate temperatures were generated to analyze the prevailing temperature conditions before and after a storm event.

Table II-2: Number of average ASSTC of each storm at all depths.

	Average ASSTC of each storm				
	30 cm	60 cm	90 cm	150 cm	Total
Winter	15	15	15	8	53
Summer	25	24	24	21	94
Total	40	39	39	29	147

Thermographs for the after-storm response for the 30 cm, 60 cm, 90 cm and 150 cm were plotted on the primary y-axis and a hydrograph of the stream stage was plotted on the secondary y-axis to show a typical after-storm substrate response during both winter and summer seasons. These thermographs and hydrographs were studied to assess the

dominant mechanics (advection or conduction) of thermal transport after a storm event. To further confirm which the dominant mode of transport is, the Peclet number $P_e = \frac{qL\rho_w C_w}{\lambda}$ (Domenico and Schwartz, 1990), which provides the ratio of advective transport to conductive transport was calculated to compliment the mode of transport realized from the analysis of the thermographs. A $P_e = 1$ is an indication of equal dominance of advective and conductive transport, whereas, $P_e > 1$ shows advective dominanted transport and $P_e < 1$ indicates conductive dominated transport. In order to test for the after-storm temperature change with depth, the average temperatures for all the after-storm responses for the 30 cm, 60 cm, 90 cm and 150 cm depths were calculated. This provided an idea about the vertical change in the amplitude of after-storm temperature response from the shallow substrate into the deeper substrate. T-test for equality of means were conducted between the pairs of 30 cm and 60 cm, 30 cm and 90 cm and 30 cm and 150 cm depths to test for significant differences in the vertical amplitude of change from the shallow substrate to the deeper substrate.

Results

Behavior of After Storm Substrate Thermal Response during Cold Periods against Warm Periods

Analysis of thermographs of all substrate after storm responses indicated that the substrate thermally responded to the storm event the same manner from mid autumn through the winter to mid spring. Late spring through summer to mid autumn also behaved similarly. Thus, there was thermal reversal in after-storm substrate thermal response in mid spring and mid autumn.

Furthermore, histograms (Figures II-4a and 4b) of the average winter and summer thermal response at all depths indicated a negative and positive skewness in the winter and summer after storm responses respectively. Both the histogram and the box plots (Figure II-5) show that the distributions of the two seasons belong to entirely two different distributions and therefore should be treated separately. Based on this observation, the data were separated into cold periods referred to as winter (late autumn, winter and early spring) and warm periods also referred to as summer (late spring, summer and early autumn), which is in line with the seasonal categorization done by Dogwiler and Wicks (2006).

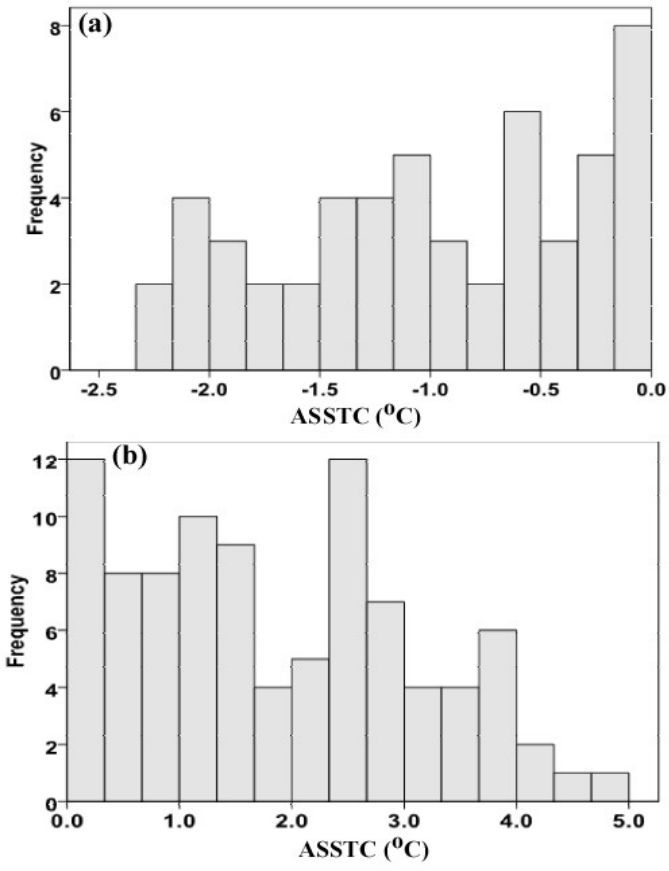

Figure II-4: Histogram of all average ASSTC of each depth from all the wells per storm during a) winter, b) summer.

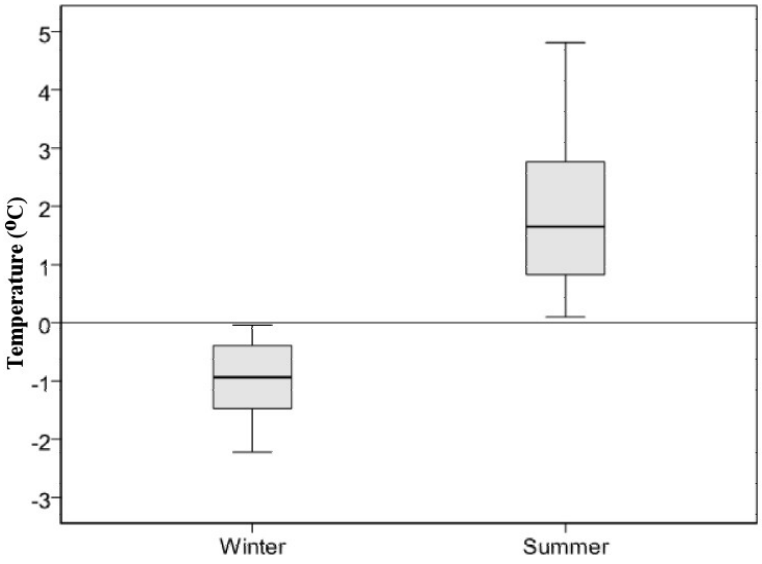

Figure II-5: Box plot of substrate after storm temperature change in all the wells. The box represents the middle 50% of the data (interquartile range). The lower and upper edges of the box represent the 25th and 75th percentiles respectively. The middle band of the box represents the median and the upper and lower whiskers represent the maximum and the minimum data respectively.

Figure II-5 gives an overview of the nature of the seasonal after storm substrate thermal response. All of the summer responses were above the 0^{o}C reference line with an average substrate after-storm spike of 1.86±1.24^{o}C during the summer. The converse, however, occurs during the winter where the responses were below the 0^{o}C reference line with an average drop of -0.99±0.68^{o}C.

The pre and peak-storm stream temperatures (Figures II-6 and II-7, Tables II-2 and II-3) show that there was no significant stream temperature changes during the winter. The summer, however, shows an average ASSTC of 1.2^{o}C. Additionally, Table II-2 and Figure II-6 show that the pre-storm stream temperatures were colder than the pre-storm substrate temperatures during the winter. After a storm, however, substrate temperatures dropped. Similarly, Table II-3 and Figure II-7 provide the pre and peak-storm temperature distributions during the summer. The pre-storm stream temperatures were

above the pre-storm substrate temperatures. The substrate, however, saw a spike in temperatures when a storm pulse came through.

Table II-3: Summary statistics of pre and peak-storm temperatures during the winter for all temperature loggers.

	Sample size (N)	**Pre-storm Temperature (°C)**		**Peak- storm Temperature (°C)**	
		Mean	Standard Deviation	Mean	Standard Deviation
Stream	17	6.32	2.71	6.61	3.03
30 cm	82	8.11	1.28	6.46	1.7
60 cm	78	9.05	1.10	7.67	1.24
90 cm	68	9.55	0.98	8.18	1.17
150 cm	26	10.11	1.18	9.76	1.32

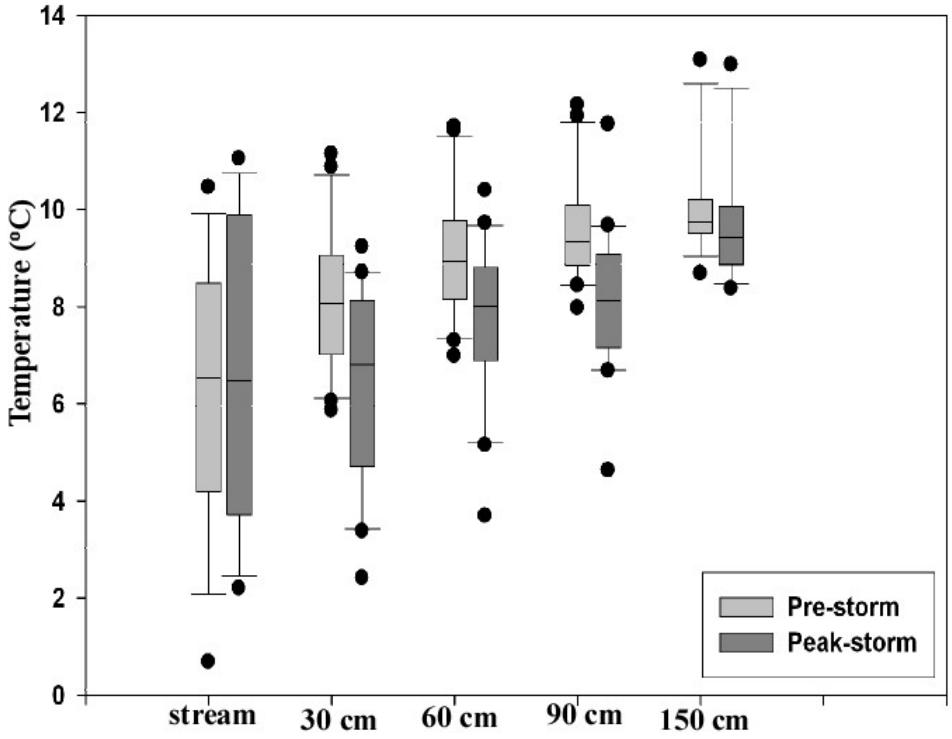

Figure II-6: a) Box plot of winter pre and peak-storm temperatures for stream and average of substrate depths for all wells.

Table II-4: Summary statistics of pre and peak-storm temperatures during the summer

	Sample size (N)	**Pre-storm Temperature (^{o}C)**		**Peak- storm Temperature (^{o}C)**	
		Mean	Standard Deviation	Mean	Standard Deviation
Stream	27	16.78	4.19	17.98	4.59
30 cm	117	14.50	3.19	16.49	4.09
60 cm	131	13.73	2.72	15.58	3.63
90 cm	118	13.01	2.39	14.80	3.41
150 cm	82	12.07	1.93	13.57	2.50

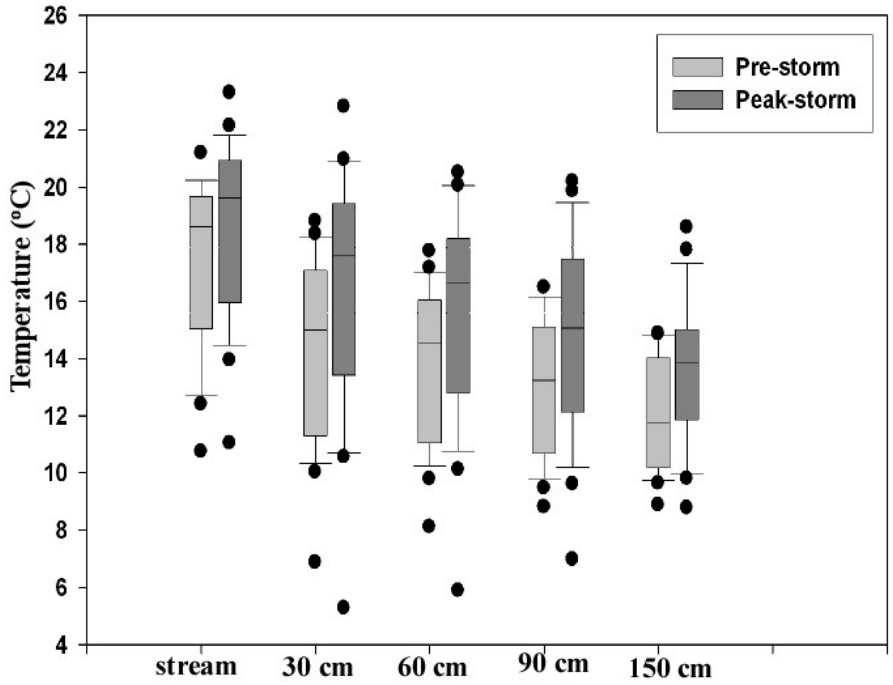

Figure II-7: a) Box plot of summer pre and peak-storm temperatures for stream and average of substrate depths for all wells.

Change of Amplitude of After Storm Substrate Thermal Response (ASSTR) with Depth

Figure II-8a and 8b provides a general trend observed during the data reduction for most of the vertical variations in the ASSTR during both winter and summer seasons. Figure II-8a shows a typical winter season ASSTR, after the storm event, both the 30 cm and 60 cm depths responded at almost the same time and have almost the same amplitude of response, i.e. -2.34^{o}C and -2.139^{o}C respectively. The 90 cm depth response, however, lagged the 30 cm and the 60 cm depth's response by 3 hours and the amplitude of response was comparatively smaller, i.e. -0.289^{o}C. The response at the 150 cm depth looks more like a diurnal response.

Figure II-8b, similarly, shows a typical warm season ASSTR. The 30 cm, 60 cm and 90 cm depths all responded at the same time after the storm event and have almost the same amplitude of responses, i.e. 3.71^{o}C, 3.044^{o}C and 3.524^{o}C respectively. The 150 cm depth, however, responded 1 hour after the 30 cm, the 60 cm and the 90 cm depth's response and had a comparatively smaller amplitude of response, 0.48^{o}C.

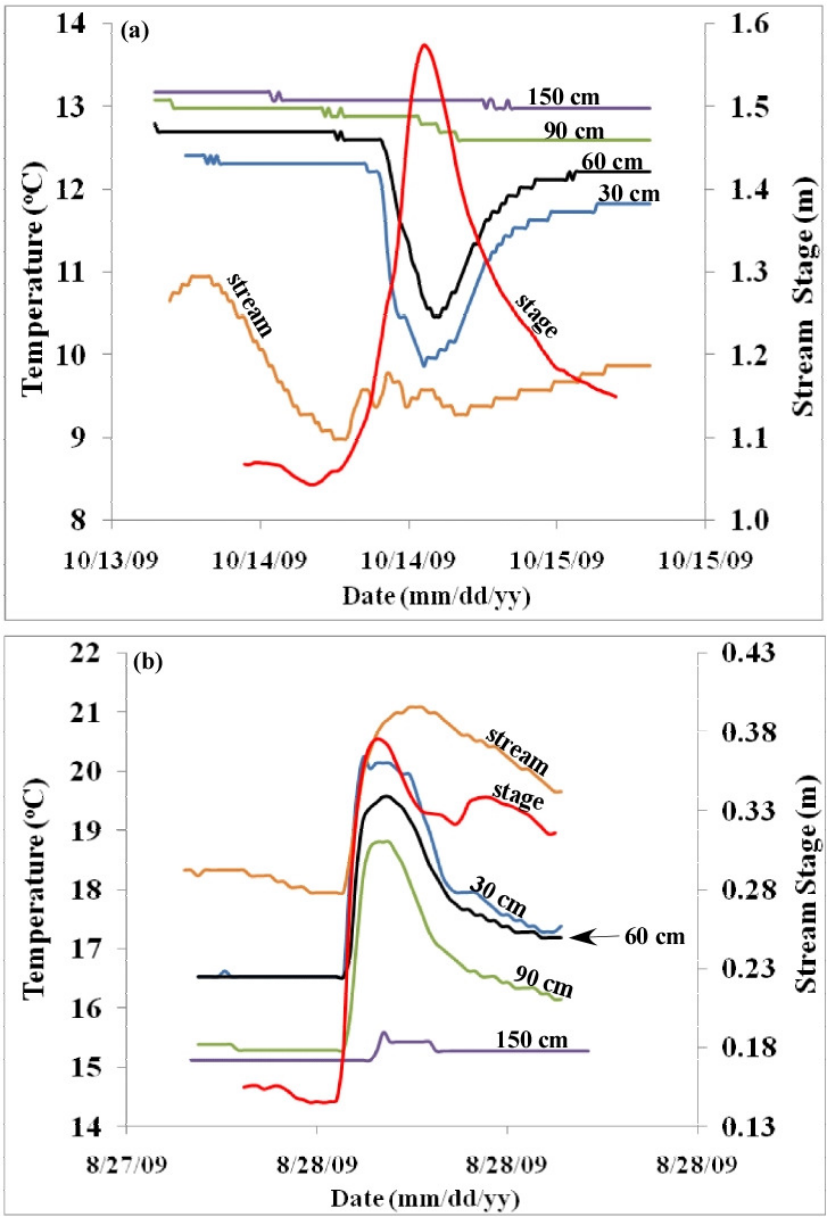

Figure II-8: a) a typical after-storm substrate temperature response during the winter, b) a typical after-storm substrate temperature response during the summer.

Using a specific discharge (q) of 0.9828 m/day estimated using the spread sheet of Hatch et al (2006). A substrate depth (L) of 1.5 m, a water density (ρ_w) of 1,000 kg/m^3, a specific heat capacity of water (C_w) of 1.0 k(cal kg^{o}C)$^{-1}$ and a thermal conductivity (λ) of 43.2 kcal(days m)$^{-1}$, a Peclet number (Pe) of 34.1 was calculated using the equation $P_e = \frac{qL\rho_w C_w}{\lambda}$ (Domenico and Schwartz, 1990).

Winter

Table II-6 provides a summary of the mean pre-storm substrate temperatures and the amplitude of ASSTC with depth during the winter. The variations indicate that the pre-storm substrate temperature increases with increasing substrate depth during the winter. The amplitude of temperature drops during the winter dampens with increasing substrate depth. The p-values of the t-test for equality of means, however, show that there are no significant differences in the dampening responses up to the 90 cm depth at the 0.05 level of significance. The 150 cm depth, however, showed a significant difference with the 30 cm depth responses at a confidence level of 0.05.

Table II-5: Mean pre-storm substrate temperature and mean amplitude of temperature change with depth during winter

Depth (cm)	Number of samples (N)	Pre-storm substrate temperature		Amplitude of ASSTC	
		Mean (^{o}C)	Std. Deviation	Mean (^{o}C)	Std. Deviation
30	17	8.23	1.94	-1.22	0.69
60	17	9.08	1.61	-1.01	0.71
90	17	10.07	1.84	-0.96	0.69
150	10	11.29	1.97	-0.55	0.44

Summer

A summary of the mean pre-storm substrate temperatures and the amplitude of ASSTC with depth for summer are provided in Table II-7. Analysis of the pre-storm temperatures reveals dampening spikes with increasing depth during the summer. The p-values of the two sample t-test for equality of means show no significant difference in the substrate spikes up to 150 cm depth at 0.05 level of significance.

Table II-6: Mean pre-storm substrate temperature and mean amplitude of temperature change with depth during summer

Depth (cm)	Number of samples (N)	Pre-storm substrate temperature		Amplitude of ASSTC	
		Mean (^{o}C)	Std. Deviation	Mean (^{o}C)	Std. Deviation
30	24	13.30	3.94	2.05	1.06
60	24	13.14	3.07	1.88	1.20
90	24	12.48	2.65	1.75	1.43
150	21	11.71	1.83	1.75	1.28

Discussion

Numerous works (e.g. Hockey *et al*., 1982; Sullican and Adams, 1991; Gu *et al*., 1999; Neumann *et al*., 2003) have shown that there is a direct relationship between air temperature and stream temperature, helping to account for the observed contrast of the after-storm substrate temperature response between the cold and warm seasons. There was not much temperature changes in the after-storm stream temperatures during the winter compared to the summer. During the summer, a warmer frontal passage is pushed into the stream, which causes a spike in the observed summer after-storm stream temperatures. The after-storm stream temperature changes also depend on the steepness of the thermal gradient between the pre-storm stream temperature and the temperature of

the incoming storm runoff. There was a drop in the after-storm substrate temperature response during the cold season and a spike during the warm season (Figure II-3), which is consistent with the works of White *et al*. (1987), Dogwiler and Wicks (2006), and Brown and Hannah, (2006).

During the winter season, the mean pre-storm stream temperature was colder than the mean pre-storm substrate temperatures (Table II-3 and Figure II-6). Results further indicate that, the pre-storm substrate temperatures increases with increasing depth during the winter, as was similarly observed by Constanz and Thomas (1996). The increase in pre-storm substrate temperature with depth is a result of the stream water maintaining a constant temperature, near 0^{o}C, due to the prevailing cold air temperature. A strong connection between the stream temperature and the upper substrate keeps the upper substrate relatively colder during the winter via the stream water temperature. As the substrate depth increases, however, the upwelling groundwater, which is warmer than the stream temperature in the winter tends to control the deeper substrate temperatures. The flux of warmer groundwater causes the pre-storm substrate temperatures to increase with increasing depth during the winter.

Analysis of stream and substrate pre and peak-storm temperatures and the box plots (Figure II-6) reveal that, pre-storm temperatures in all the wells during the winter were above the 8^{o}C. After the storm, however, substrate temperatures dropped to below/about 8^{o}C. The drop in the after-storm substrate temperature is due to the increase vertical hydraulic gradient during high hydrologic flow, which increases the vertical hydraulic head, which also increases the flux of the stream water into the streambed. As the relatively colder stream water inundates the substrate, there is mixing and thermal

homogenization of the colder stream water with the relatively warmer substrate water. For there to be thermal equilibrium during the mixing of the warmer pre-storm substrate temperature with the incoming colder stream temperature, the substrate temperatures will have to drop, which explains the observed drop in the ASSTC during winter season.

Similarly, during the summer season, the mean pre-storm stream temperature was higher than the mean pre-storm substrate temperatures (Table II-4 and Figure II-7). To further clarify the substrate variation, Table II-6 indicates that, the pre-storm substrate temperatures dampen with increasing depth during the summer season, which is consistent with the observation by Constanz and Thomas (1996) and Evans and Peets (1997). The warmer pre-storm stream water is due to diurnal heating of the stream water from the sun's radiation (Cassie, 2006) and the warmer frontal passage (Dogwiler and Wicks, 2006). The upper substrate, however, has a strong temperature connection with the stream water, which makes the upper substrate relatively warmer via the stream water. As the substrate depth increases, however, the upwelling groundwater, which is colder than the stream water in the summer, tends to control the temperatures at the deeper substrate, and therefore, the dampening of the substrate temperatures with increasing depth during the summer.

A study of the box plots (Figure II-7) show that, pre-storm temperatures in all the wells during the summer were below 15^{o}C. After the storm, however, all substrate temperatures spiked to above/about 15^{o}C. The spike in the after-storm substrate temperature is due to the influx of the relatively warmer stream water into the substrate, which leads to mixing and thermal homogenization of warmer stream water with relatively colder substrate water.

The works of Suzuki (1960), Stallman (1965), Wierenga *et al*. (1970) and Nightingale (1975) revealed that vertical heat transfer into the streambed is controlled predominantly by advective and to a lesser extent by conductive transport. Figure II-8a and II-8b shows the extent of the storm water flux into the streambed (wetting front) and the rapid and slow thermal transmission due to advective and conductive controlled transports respectively. The vertical flux of the stream water into the streambed transmitted the heat rapidly up to the 60 cm depth with bigger amplitude of response as the storm pulse came through (Figure II-8a), which is an indication of advection dominated heat transfer up to the 60 cm depth (e.g. Constanz and Thomas, 1996; Evans and Peets, 1997). It also indicates a 60 cm wetting front of the storm. The sharp temperature change at the 60 cm depth creates a high thermal gradient between the 60 cm and the deeper substrate, which induces conduction of heat from the 60 cm to the 90 cm depths. The small amplitude of response and the longer lag time for the 90 cm response, however, was due the conductive mode of heat transport. Figure II-8b, similarly, shows an advective dominated heat transport and a wetting front up to the 90 cm depth, with a subsequent conduction dominated heat transfer from the 90 cm to the 150 cm depth during the summer season. The Peclet number of 34.1 also confirms the advective dominated transport after a storm. Thus, one can eliminate the idea of using the pre-storm thermal gradient (which controls conductive transport) to normalize the ASSTC.

A dampening of after-storm substrate thermal response with increasing substrate depths occurred following both cold and warm season storms (Table II-5 and II-7), which is consistent with the findings of Dogwiler and Wicks (2006) and Brown and Hannah (2006).

The dampening of thermal response with increasing depth is because the after-storm substrate response is mainly due to thermal gradient between the pre-storm stream water and pre-storm substrate temperatures. The steeper the thermal gradient, the bigger the amplitude of the ASSTC during mixing and thermal homogenization of the stream water with the hyporheic water. As the initial stream water percolates into the substrate, at the 30 cm depth (upper substrate) there is a steeper thermal gradient, and therefore, the 30 cm depth must take a bigger response in order to thermally equilibrate with the stream water. As the stream water percolates deeper, it has been altered having mixed with the water at 30 cm and some of the homogenized water into the deeper substrate. Additionally, the streambed sediments also act as a mechanical filter to the surface thermal inputs (Vervier *et al*., 1992). The stream water that gets to the 60 cm depth, therefore, has a muted temperature gradient. Thus, the 60 cm depth will experience a smaller spike during mixing and thermal equilibration with the stream water. The same procedure is repeated between the 60 cm and the 90 cm and between the 90 cm and the 150 cm. The muted thermal gradient with increasing substrate depth accounts for the dampening ASSTC with increasing substrate depth.

Test of equality of means from the 30 cm to the 150 cm depths for both cold and warm seasons were run to help further assess the significance in the variations of ASSTC with increasing depth. Though there was dampening of ASSTC with increasing depth, the p-values reveal that there were no significant differences in the summer ASSTC from the 30 cm to the 150 cm depths. During the winter, however, significant difference was observed at the 150 cm depth with the 30 cm depth response. The similarity in the summer ASSTC with increasing depth as compared to the winter is as a result of the

summer warm storm water penetrating the streambed deeper than the winter cold storm water. The work of Constantz (1998) and Baskaran *et al*. (2009) showed an increase in seepage rate with increasing temperature due to changes in water density and dynamic viscosity.

Conclusion

The aim of this study was to assess the impact of storm events on thermal anomalies in the streambed. Various aspects of ASSTC such as seasonal and vertical variations were addressed to meet the object of this study. In totality, there were seasonal differences in the ASSTC with winter substrates responding to storm event with drops, whereas, the summer substrate responded with spikes, which implies a seasonal thermal reverse in after-storm substrate response. The seasonal reverse in response will inform resource managers as to the type of acute temperature changes to expect in the substrate after a storm event given a particular season. The depth of wetting front of a storm event determines the depth to which advective transport controls thermal transmission into the substrate. The acute temperature change at the depth of the wetting front creates a steep thermal gradient, which induces conductive transport, which further propagates heat into the deeper substrate. Nonetheless, advection dominates ($P_e = 34.1$) the overall vertical heat transport after a storm event. In addition to advection and conduction controlling vertical temperature transmission into the substrate, the amplitude of the vertical responses dampens with increasing depth. There are however, no significant differences

in the dampening responses with increasing depth in the summer, whereas, the winter response showed significant difference at 150 cm depth at 0.05 level of significance.

References

Anderson MP. 2005. Heat as a Ground Water Tracer. *Ground Water* **43**: 951-968. DOI: 10.1111/j.1745-6584.2005.00052.x.

Arntzen EV, Geist DR & Dresel PE (2006) Effects of fluctuating river flow on groundwater/surface water mixing in the hyporheic zone of a regulated, large cobble bed river. *River Res. Applic*. **22**: 937-946

Baskaran S, Brodie RS, Ransley T & Baker P (2009) Time-series measurement of stream and sediment temperature for understanding river-groundwater interactions: Boarder Rivers and Lower Richmond Catchments, Australia. *Australian Journal of Earth Sciences*, **56**: 21-30

Boulton AJ, Findlay S, Marmonier P, Stanley EH & Valett HM (1998) The functional significance of the Hyporheic zone in streams and rivers. *Annual Review of Ecology and Systematics* **29**: 59–81.

Bouyoucos G (1915) Effects of temperature on some of the most important physical processes in soils. MIchgan College of Agriculture Technical Bulletin 24.

Brown LE and Hannah DM (2005) Spatial and temporal water column and streambed temperature dynamics within an alpine catchment: Implications for Benthic communities. *Hydrol. Processes*, **9**: 1585-1610.

Brown LE and Hannah DM (2006) Alpine stream temperature response to storm events. *Journal of Hydrometeorology*, **8**: 952-967.

Brunke M & Gosner T (1997) The ecological significance of exchange processes between rivers and groundwater (special review). *Freshw Biol* **37**:1–33

Caissie D (2006) The thermal regime of rivers: A review. *Freshwater Biol*., **51**: 1389-1406.

Conant B Jr. (2004) Delineating and Quantifying Ground Water Discharge Zones Using Streambed Temperatures. *Ground Water* **42**: 243-257.

Constantz J (1998) Interaction between stream temperature, streamflow and

groundwater exchanges in alpine streams. *Water Resour. Res*., **34**: 1609-1616.

Constantz J and Thomas CL (1996) The use of streambed temperatures profiles to estimate depth, duration, and rate of percolation beneath arroyos. *Water Resour. Res*., **32**: 3597- 3602, doi:10.1029/96WR03014.

Constantz J, Cox MH, Su GW (2003) Comparison of heat and bromide as ground water tracers near streams. *Ground Water* **41**: 647-656.

Curry RA, Gehrels J, Noakes DLG & Swainson R (1994) Effects of river flow fluctuations on groundwater discharge through brook trout. Salvelinus fontinalis, spawning and incubation habitats. *Hydrobiologia:* 121-134.

Dogwiler T & Wicks C (2006).. Thermal variation in the hyporheic zone of a karst Stream *International journal of Speleology* **35**: 59-66.

Dole-Olivier MJ & Marmonier P (1992) Effects of spates on the vertical distribution of the interstitial community. *Hydrobiologia* **230**:49–61

Dole-Olivier MJ, Marmonier P, Beffy JL (1997) Response of invertebrates to lotic disturbance: is the hyporheic zone a patchy refugium? *Freshw Biol* **37**:257–276

Evans EC & Petts GE (1997) Hyporheic temperature patterns within riffles. *Hydrol Sciences-Journal,* **42(2),** 199–213.

Evans EC, McGregor GR and Petts GE (1998) River energy budgets with special reference to river bed processes. *Hydrol Processes,* **12,** 575–596.

Fraser BG, Williams DD & Howard KWF (1996) Monitoring biotic and abiotic processes across the hyporheic/groundwater interface. *Hydrogeology Journal* **4(2)**: 36-50.

Galloway B J & Kieffer JD (2003) The Effects of an Acute Temperature Change on the Metabolic Recovery from Exhaustive Exercise in Juvenile Atlantic Salmon (Salmo salar). *Physiological and Biochemical Zoology* **76(5)**: 652–662.

Glennon RJ (2002) *Water Follies: Groundwater Pumping and the Fate of America's Fresh Waters*: Washington D.C., Island Press, 354 p.

Grimm NB & Fisher SG (1984) Exchange between interstitial and surface water: Implications for stream metabolism and nutrient cycling. *Hydrobiologia* **111**, 219-228.

Grimm NB, Valett, HM, Stanley EH & Fisher SG (1991) Contribution of the hyporheic zone to the stability of an arid-land stream. *Verhandl Int Vereinig Theoret Ange Limno*l **24**:1595–1599

Gu R, McCutcheon R and Chen CJ (1999) Development of weather-dependent flow requirements for river temperature control. *Environ. Manage. (N.Y.),* (**24**): 529–540

Hatch CE, Fisher AT, Ruehl C, Revenaugh JS and Constantz J (2006) Quantifying surface water-groundwater interactions using time series analysis of streambed thermal records: Method development. Water Resources Research, **42(10)**

Hockey JB, Owens IF and Tapper NJ (1982) Empirical and theoretical models to isolate the effect of discharge on summer water temperature in the Hurunui River. *J. Hydrol. (New Zealand),* **21**: 1–12.

Hannah DM, Gurnell AM and McGregor GR (1999) Identifying links between large-scale atmospheric circulation and local glacier ablation climates in the French Pyrénées. *IAHS Publ.,* **256,** 155–164.

Hannah DM, Malcom IA, Soulsby C, & Youngson AF (2004) Heat exchanges and temperatures within a salmon spawning stream in the Cairngorms, Scotland: Seasonal and subseasonal dynamics. *Riv. Res. Apps*. **20**: 635-652.

Hedin LO, von Fischer JC, Ostrom NE, Kennedy BP, Brown MG and Robertson GP (1998), hermodyamic constraints on nitrogen transformations and other biogeochemical processes at soil-stream interfaces, *Ecology*, **79(2)**: 684-703.

Hondzo M & Stefan HG (1994) Riverbed heat conduction prediction. *Wat. Resour. Res.* **30**: 1503-1513.

Hondzo M & Wang H (2002) Effects of turbulence on growth and metabolism of periphyton in a laboratory flume. *Water resources Research* **38**: 1277. Doi: 10.1029/2002WR001409.

Hunt RJ, Strand M and Walker JF (2006) Measuring groundwater-surface water interaction and its effect on wetland stream benthic productivity, Trout Lake Watershed, northern Wisconsin, USA, *J. Hydrol*. **320**, 270-384.

Hynes HBN (1970) *The Ecology of Running Waters.* Liverpool University Press, Liverpool, UK.

Hynes HBN (1983) Groundwater and stream ecology. *Hydrobiologia* **100,** 93-99.

Hynes HBN, Williams DD & Williams NE (1976) Distribution of the benthos within the substratum of a Welsh mountain stream. *Oikos* **27,** 307-310.

Karlsson OM, Richardson JS & Kiffney PM (2005). Modeling organic matter dynamics in headwater streams of south-western British Columbia, *Canada. Ecological Modeling* **183**: 463 – 476

Kenoyer GJ and Anderson MP (1989) Groundwater's dynamic role in regulating acidity and chemistry in a precipitation-dominated lake. *J. Hydrol*., **109**: 287-306.

Kishi D, Murakami M, Nakano S & Maekawa K (2005) Water temperature determines strength of top-down control in a stream food web. *Freshwater Biology* **50**: 1315 – 1322.

Lapham WW (1989) Use of temperature profiles beneath streams to determine rates of vertical ground-water flow and vertical hydraulic conductivity. USGS Water-Supply Paper 2337. Reston, Virginia: USGS.

Lee DR (1985) Method for locating sediment anomalies in lake beds that can be caused by groundwater inflow. *J. Hydrol*., **79**:187 193.

Malard F, Mangin A, Uehlinger U, Ward JV (2001) Thermal heterogeneity in the hyporheic zone of a glacial floodplain. *Canadian Journal of Fisheries and Aquatic Sciences* **58**: 1319-1335. DOI: 10.1139/cjfas-58-7-1319.

Malcom IA, Soulsby C, Youngson AF, Hannah DM, McLaren IS, and Thorne A (2004) Hydrological influences on hyporheic water quality: Implications for salmon err survival. *Hydrol. Processes,* **18**: 1543-1335.

Morin A, Lamoureux W & Busnarda J (1999) Empirical models predicting primary productivity from chlorophyll and water temperature for periphyton and lake and ocean phytoplankton. *Journal of the North American Benthological Society* **18**: 299-307.

Nightingale HI (1975) Ground-water recharge rates from thermometry. *Ground Water*, **13**: 333±344.

Peterson EW & Sickbert TB (2006) Stream water bypass through a meander neck, laterally extending the hyporheic zone. *Hydrogeology Journal* **14**: 1443-1451. DOI: 10.1007/s10040-006-0050-3.

Poole GC & Breman CH (2001) An ecological perspective on in-stream temperature; natural heat dynamics and mechanisms of human-caused thermal degradation. *Environmental Management* **27**: 787- 802.

Poole WL & Stewart KW (1976) The vertical distribution of macrobenthos within the substratum of the Brazos River, Texas. *Hydrobiolobia* **50**, 151-160.

Shepherd BG (1984) Predicted impacts of altered water temperature regime on Glendale Creek pink fry. *Canadian MS Report on Fisheries and Aquatic Science, no.* 1782

Silliman SE & Booth DF (1993) Analysis of time-series measurements of sediment

temperature for identification of gaining vs. losing portions of Juday Creek, ndiana. *Journal of Hydrogeology* **146**: 131-148.

Silliman SE, Ramirez J & McCabe RL (1995) Quantifying downflow through creek sediments using temperature time series: One-dimensional solution incorporating measured surface temperature. *Journal of Hydrogeology* **167**, 99-119.

Soulsby C, Malcolm IA & Youngson AF (2001) Hydrochemistry of the hyporheic zone in a salmon spawning gravels: a preliminary assessment in a degraded agricultural stream. Regulated Rivers: *Research & Management* **17**: 651-665.

Stallman RW (1965) Steady one-dimensional fluid flow in a semi-infinite porous medium with sinusoidal surface temperature, *J. Geophy. Res.*, **70**, 2821-2827.

Stanford JA & Ward JV (1993) An ecosystem perspective of alluvial rivers: connectivity and the hyporheic corridor. *J North Am Benthol Soc* **12**:48–60

Stonestrom DA and Constantz J (2004) Heat as a tool for studying the movement of ground water near streams. USGS Circular 1260. Reston, Virginia: USGS.

Suzuki S (1960) Percolation measurements based on heat flow through soil with special reference to paddy fields, *J. Geophys. Res.*, **65**: 2883-2885.

Valett HM, Fisher SG & Stanley EH (1990) Physical and chemical characteristics of the hyporheic zone of a sonorant desert steam. *J. North AM. Benthol. Soc*. **9**: 201-215

Vervier P, Gilbert J, Dole-Olivier MJ & Marmonier P (1992) A perspective on the permeability on the surface freshwater-groundwater ecotone. *J. North Am. Benthol. Soc.* **11**, 93-102.

Ward JV (1985) Thermal characteristics of running waters. *Hydrobiologia* **125**: 31-46

Wierenga PJ, Hagan RM and Nielsen DR (1970) Soil temperature profiles during infiltration and redistribution of cool and warm irrigation water, *Wat. Resour. Res*., **6**, 130-238.

Wroblicky GJ, Campana ME, Valett HM & Dahm CN (1998) Seasonal variations in surface-subsurface water exchange and lateral hyporheic area of two stream-aquifer systems. *Water Resources Research* **34**: 317-328

White DS, Elzinga CH, Hendricks SP (1987) Temperature patterns within the hyporheic zone of a northern Michigan river. *Journal of North American Benthological Society* **12**: 48-60.

CHAPTER III

PREDICTIVE MODEL APPROACH

Abstract

The significance of heat in stream and hyporheic exchange and its impact on lotic system is far reaching, and one event that affects temperature in the hyporheic zone (HZ) is a storm (high flow) event. The area of research in fitting predictive models to simulate After-Storm Substrate Temperature Change (ASSTC) remains completely unstudied and the focus of this paper is to help bridge this research gap. Six (6) wells were installed along a 25 m straight stretch of Little Kickapoo Creek (LKC) at Mclean County, Illinois, USA. The results of this study indicate that during the winter, the pre and peak-storm stage and amplitude of stream temperature change control the ASSTC, whereas, the amplitude of storm and pre and peak-storm stream temperature were the relevant controlling parameters during the summer. The entire year's ASSTC however, are controlled by the pre-storm stage, amplitude of storm and pre and peak-storm stream temperatures. The correlations of the amplitude of storm with ASSTC indicate that heavy storms do not necessarily lead to an increase in ASSTC. Rather, the ASSTC depends on other factors such as the pre-storm stage and pre-storm thermal gradient between the temperature of the stream and the pre-storm substrate temperature. A simple curvilinear regression model based on the amplitude of storm and the peak-storm stream temperature was fitted to simulate ASSTC for the entire year. The model will aid resource managers in the investigation and management of aquatic ecosystem within the HZ after a storm event given the importance of the impact of acute temperature change on aquatic stability.

Introduction

Streambed is an important component of lotic ecosystems (Ward, 1989) which controls the flux of energy and materials between surface and groundwater systems (Gilbert *et al.,* 1990) serving as a mechanical filter (Vervier et al., 1992) that controls surface thermal inputs via conductive, convective and advective modes of thermal transport. The interface underneath the streambed where groundwater and surface water mix or where surface water infiltrates into biologically active near stream sediments is known as the hyporheic zone (HZ) (Boulton et al., 1998; Conant, 2004; Hayashi and Rosenberry, 2002).

The significance of temperature in the HZ cannot be overemphasized since it serves as an important biological variable (Hynes, 1970). Vannote & Sweeney (1980) revealed that HZ temperature pattern may have a remarkable influence on the distribution of aquatic invertebrate as different species have different thermal optima. Lateral, longitudinal and vertical temperature patterns in the stream and streambed determines the distributions and life cycles of benthic and macroinvertebrates (Standford and Ward, 1988). The direction of acute temperature changes is important, Galloway and Kieffer (2003) observed that acute decrease and increase in HZ temperature affect osmotic balance of salmon; while acute increase in temperature enhanced salmon recovery an acute decrease in temperature slows the recovery of various muscle and blood metabolites.

Additionally, the HZ serves as a hatchery for salmonid and invertebrate eggs (Hynes, 1983; Shepherd, 1984) and serves as a refuge for invertebrate and larval fish during spates (Hynes et al., 1976; Poole & Stewart, 1976). The sedimentological composition of

the HZ can affect the permeability and porosity of the substratum which may lead to significantly different HZ temperature patterns (Wickett, 1954; Ringler & Hall, 1975; Evans *et al.,* 1995). The HZ sediments have a buffering capacity which shields the hyporheic water from direct atmospheric contact serving as a potential heat source/sink for channel water (Evans & Peets, 1997).

River system heat transfer is complex; advected by in/out flowing stream discharge, evaporated water, groundwater up/downwelling, tributary inflows and precipitation (Hannah *et al.*, 2004). Precipitation inundates the stream and streambed with enormous quantity of thermally unequilibrated water (Dogwiler and Wicks, 2006) which can cause changes in stream temperature due to direct inputs and by inducing runoff from/via various hydrological stores/pathways (Kobayashi et al., 1999; Brown and Hannah, 2007). The amplitude of after-storm temperature change corresponds to the intensity of the precipitation and the amplitude of response decays with increasing substrate depth (Dogwiler & Wicks, 2006; Brown and Hannah, 2007).

Numerous research works have focused on using external climatic factors to fit predictive models to simulate stream temperatures. Major external drivers that determine how much heat is added or taken from a river thermal system are direct and indirect solar radiation, air temperature, groundwater inputs, and wind speed (Sullican and Adams, 1991). Specifically, Neumann *et al.,* (2003) used air temperature and flow rate to develop a linear regression model to predict daily maximum stream temperatures during low flow periods. Mitchell (1999) used pre-harvesting stream temperatures to build a model to predict post-harvesting stream temperatures after the removal of a riparian canopy cover. Similarly, Mellina *et al*., (2002) build a cooling model (difference between upstream and

downstream daily mean temperatures) from the upstream maximum temperature and canopy cover after a clearcut logging. Irrespective of the importance of HZ acute temperature changes on aquatic and ecological stability which is exactly the condition after a storm event, the area of research in fitting a predictive model to simulate After Storm Substrate Temperature Change (ASSTC) to help in the management of aquatic organism, notably in the HZ, remains completely unstudied.

The focus of this paper is to help address the above research gap by fitting a predictive model to a 1 year data from a low-gradient third-order sand and gravel bedded stream. This aim is achieved by exploring the following specific objectives: (1) to explore the relevant factors/parameters that control ASSTC; (2) using the relevant parameters to fit an ASSTC model(s) to help simulate substrate thermal responses to a storm event. This model will provide resource managers with a tool in predicting ASSTC to help in the investigation and management hyporheic organisms.

Methodology

Study Locality

A 25 m straight stretch along the Little Kickapoo Creek (LKC) located in Mclean County in Central Illinois, USA, was selected for the purposes of this investigation (Figure III-1). The LKC is a low gradient third-order perennial gaining stream with a general gradient of 0.002 (Peterson and Sickbert, 2006).

Three geologic units make up the alluvial valley along the stretch of the study site (Figure III-1). These include the Wedron Formation (WF), the Henry Formation (HF), and the Cahokia Formation (CF), listed from oldest to youngest. The WF acts as a lower

confining unit to the HF, being a clay-rich low-permeable till with some interstitial sand and gravel deposited by past glacial activity.

The stream cuts through the CF and the channel runs through the HF. The main aquifer is the HF because of its poorly sorted gravels and sands, with an average hydraulic conductivity of 10m/day and an average thickness of 5-7 m in the outwash valley. The CF lies above the HF and it is made up of silt and clay, with some interstitial sand lenses. Repeated flooding of LKC formed the CF with an average thickness of approximately 2 meters across the outwash valley. The CF is not considered a confining unit because of the presence of macro porosity and high level of connectivity between LKC and HF.

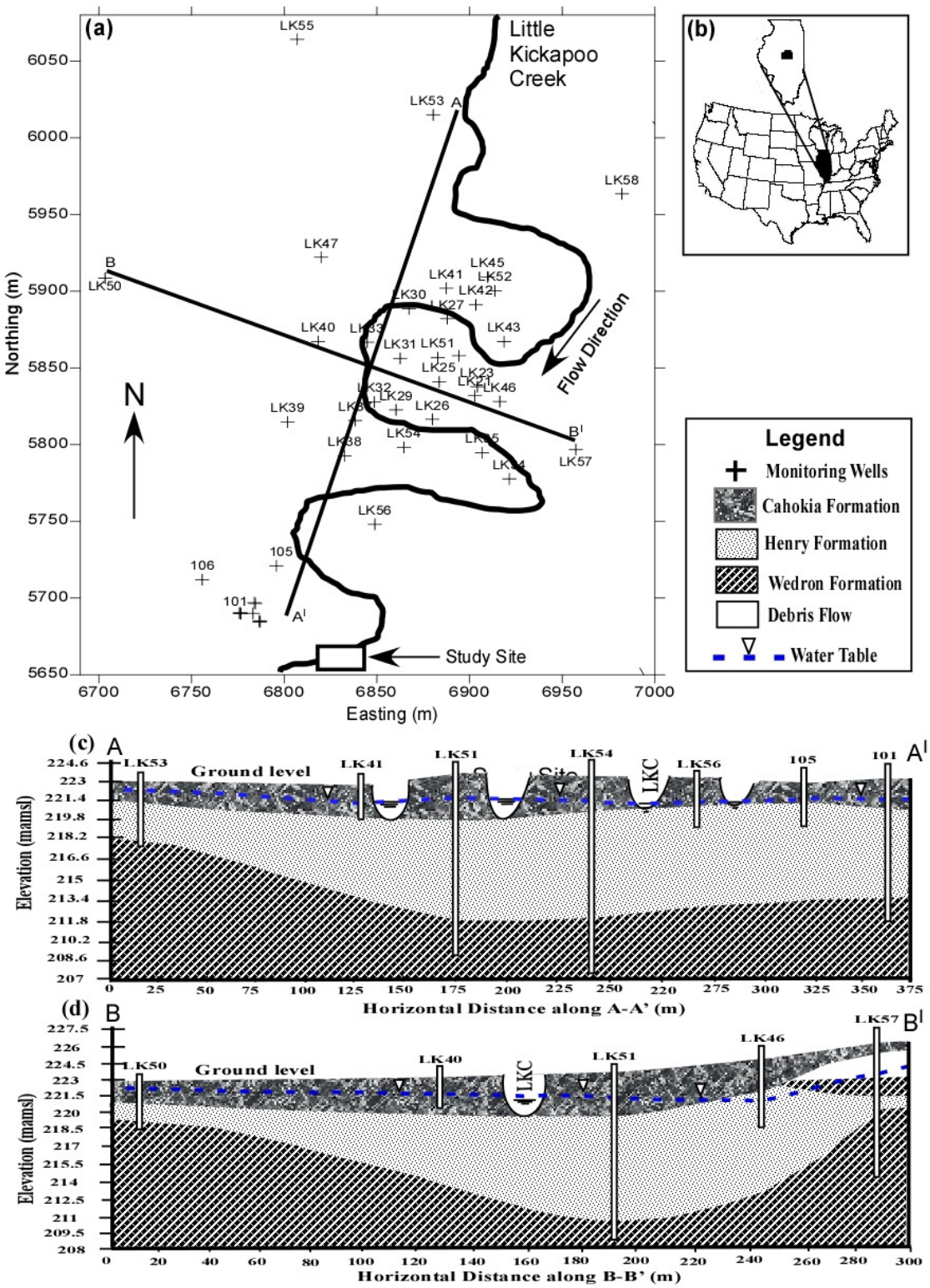

Figure III-1: a) Figure showing an aerial map of the Randolph well field study area with cross section line locations, b) the US state map showing Illinois State and McLean County, c and d) Cross sections along lines A-A^{1} and B-B^{1} respectively.

Climatic Setting

Central Illinois has a humid continental climate with cold winters and warm summers. Between the periods of 1950 to 2002, the annual mean temperature was 11.2°C (Peterson and Sickbert, 2006). Specifically, Bloomington, IL climate is warm during summer when temperatures tend to be in the 20 - 30^{o}C range and cold during winter when temperatures are between –1 to –10^{o}C. July is the warmest month of the year with an average maximum temperature of 30^{o}C, while January is the coldest month with an average minimum temperature of –10^{o}C. There are moderate temperature variations between night and day during the summer with a variation of about ± 6.1^{o}C, and an increase variation between night and day temperatures during winter with an average difference of ±7.8^{o}C. The total annual precipitation at Bloomington is 952.75 mm with the wet season in spring and the dry season in winter (Table III-1). All the data are available at the Bloomington Waterworks Weather Station, which is about ten miles upstream of the study site. Ants damaged the weather station set up at the study site.

Table III-1: Annual precipitation of Bloomington

Month	Jan	Feb	Mar	April	May	June	July	Aug	Sep	Oct	Nov	Dec	Annual
Millimeters	36.6	42.4	76.5	90.9	108.5	101.4	95.8	93.0	84.6	66.3	81.5	73.4	952.8

Data Collection

A well grid was set up at the selected study site along riffles within the LKC using a drive-point installation method. The site consisted of six wells (W1, W2, W3, W4, W5 and W6) creating longitudinal profile lines along the stream channel (Figure III-2). Temperature loggers were positioned at multiple depths of 30 cm, 60 cm, 90 cm, and 150

cm within each 6.35 cm PVC well (Figure III-3). Each chamber was separated using foam sealant to prevent vertical mixing of the water in the well.

Separate temperature loggers were attached to W1 and W6 to record upstream and downstream surface water temperatures respectively. A stilling well was located at the bank of the stream in line with well 2 to record the stream stage (Figure III-2). All loggers were programmed to record temperatures at 15-minute intervals due to time needed for the loggers to respond to changes in temperature within the system. Data were collected from February 2009 until March 2010. A total of 41 storms were recorded during this period, making up of 24 storms during the summer period (later spring to early autumn) and 17 storms during the winter period (later autumn to early spring).

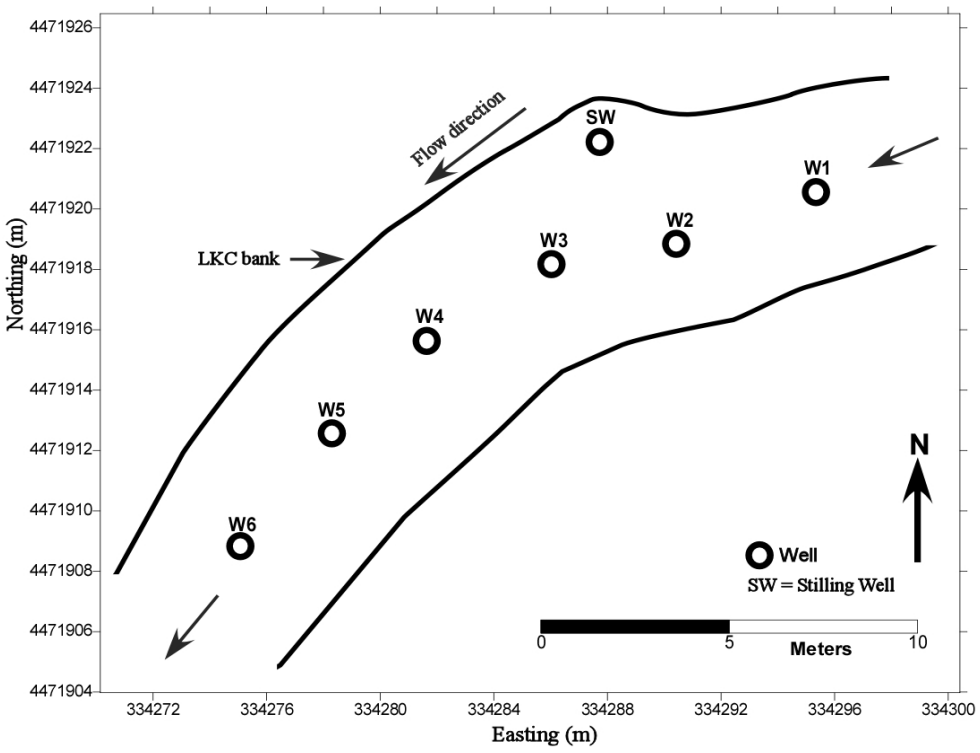

Figure III-2: Birds-eye view of well setup in the stream channel. The numbers indicate respective well names used.

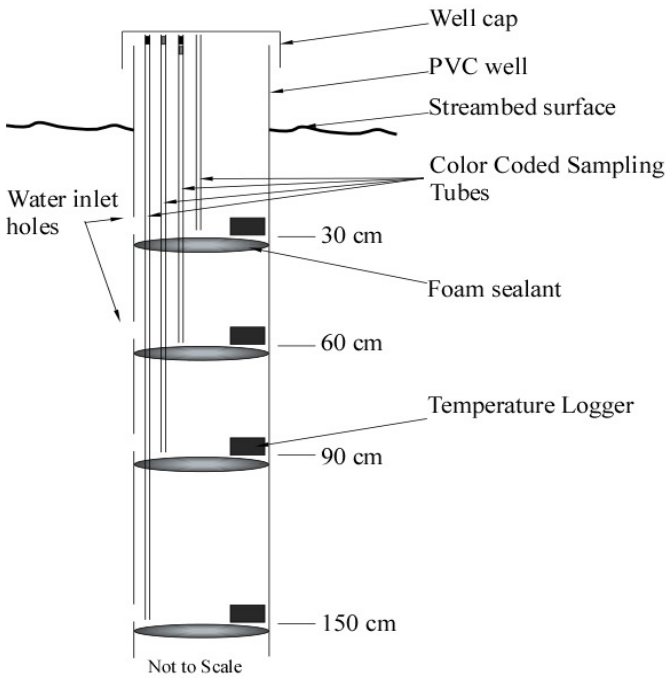

Figure III-3: Detailed view of individual well design

Data Reduction

A hydrograph of the stream stage data was plotted to identify periods of high flow and to extract the storm events. The extracted storm events were compared with precipitation data collected from the US weather service for Bloomington in order to separate storm events from diurnal rises. The amplitude of storm was calculated by subtracting the pre-storm (baseflow) stream stage from the peak-storm stream stage. Thermographs for all loggers in all wells at the various depths and the stream were also plotted and compared to the hydrographs to locate the streambed and stream thermal responses as a result of the storm pulse coming through. The amplitudes of the streambed and stream thermal pulses due to the storm pulse were extracted by subtracting the pre-storm temperature from the peak-storm temperature to get the After-Storm Substrate

Temperature Change (ASSTC). The averages of all the ASSTC for each depth in all wells were calculated to represent the ASSTC for a particular storm for that depth. This was done to avoid redundancy of data and to get rid of noise in the data.

Methods of Controlling Parameters

For the research question of comparing the important factors that affect ASSTC most, a normality test was first run on all the dependent variables (ASSTC at 30 cm, 60 cm, 90 cm and 150 cm) and the independent variables (amplitude of storm, pre and peak-storm stage, pre and peak-storm stream temperature, amplitude of stream temperature change) to test for normality in the data. There was normality in the data and therefore, the parametric approach (Pearson's coefficient of correlation) was used for the analysis. Details on the calculations of the Pearson's coefficient of correlations could be found in Tabachnick and Fidell (1989).

In order to test for the most influential independent variable on the ASSTC, a test of correlation between the independent variables (IV) were ran against the dependent variables (DV) for the various depths (30 cm, 60 cm, 90 cm, and 150cm) to determine their correlation coefficients (r). The coefficient of correlation between ASSTC and each variable's pre and peak-storm temperature/stage and the amplitude of change were compared. In instances where the pre and peak-storm temperature/stage values correlated better with ASSTC than the amplitude of the change, the pre and peak-storm variables were considered as the controlling parameters. When the amplitude of change correlated better with ASSTC, however, only the amplitude of the change was considered the controlling variable since it has a component of both the pre and peak-storm responses.

This was done to avoid multicollinearity, where there is high correlation among the retained independent variables thereby overestimating the influence of a single factor in contributing to the observed substrate temperature change. The coefficient of determination (r^2) was calculated to determine the percentage of the ASSTC that is explained or accounted for by each variable. Scatter plots of the controlling IV against the 30 cm ASSTC were plotted to provide a visual discernment of the observed relationship.

Methods of Predictive Model Construction

The essence of a regression model is to develop an equation from a set of data (IVs) that presents the best prediction of the dependent variable (DV). The simplest form of the equation being a linear equation in the form:

$$ASSTC = A + B_1X_1 + B_2X_2 + \ldots\ldots\ldots + B_kX_k$$

where ASSTC = After-storm substrate temperature change, A = constant of prediction, B_1, B_2, ……, B_k = coefficients and X_1, X_2, ……, X_k = independent predictors (Tabachnick and Fidell, 1989).

All the 41 storms were randomly separated into two subsets, one for model development and the second for model verification (Table III-2). The total for all depths is not exactly four times the total storms because some storms could not penetrate to either the 90 cm or 150 cm depths, and therefore there was no reading for either the 90 cm or the 150 cm for those storms.

Table III-2: Number of storms for model development and model verification.

	Winter storms	Summer storms	Total storms	Total for all depths (N)
Model Development	10	15	25	90
Model Verification	7	9	16	60
Total	17	24	41	150

The model development data variables were tested for normality, for skewness, and for outliers. Based on the skewness and the shapes of the distribution curves for the IVs and DV, the variables were transformed to stabilize the variances using the logs and square root of the variables.

A predictive model was built from the transformed variables using the stepwise regression procedure. The stepwise method uses statistical criteria to retain only variables that are significant at $p = 0.05$ (Mellina *et al*., 2002). The developed model was diagnosed by investigating the performance of the predictive model by looking at the following diagnostic features, normal probability plot, histogram of the regression standardized residual with normality plot, and scatter plot of regression unstandardized residual against the transformed ASSTC were plotted. This provides a test of assumption of multivariate normality, linearity, and homoscedasticity between the predicted dependent values and the errors of prediction.

Mahalanobis and Cook's distances were used to test for multivariate outliers. When the Mahanabolis distance is smaller than the critical value given the number of independent variables it means there is no multivariate outliers. Similarly, Cook's distance less than 1 is an indication of no multivariate outlier. That is, no single variable is overly controlling the outcome of the analysis (prediction model).

Durbin-Watson statistic was used to test for the presence/absence of autocorrelation or dependence of errors in the residuals. A Durbin-Watson value significantly less than 2 indicates a positive autocorrelation and significantly greater than 2 is an indication of a negative autocorrelation in the residuals.

Cross correlations between the retained independent variables were used to check for multicollinearity among the retained variables. This was to ensure that there was no high correlation between the retained independent variables thereby overestimating the influence of a single factor in the analysis.

Finally, the verification data were used to test the ability of the developed model to predict future events in the stream. The model was used to simulate ASSTC of the model verification data which was not used in fitting the model. A regression was performed between the measured and the predicted values in order to compute the equation of the line of best fit and to estimate the adjusted R^2. The line of best fit of a perfect model should go through the origin. The adjusted R^2 will provide an idea about how accurate the model is able to simulate the measured values. A scatter plot showing the line of best fit and the 95% prediction interval of the predicted against the measured ASSTC was plotted to provide a visual discernment of the ability of the model to predict a future event.

Results

Predominant Parameters Controlling ASSTC

Winter

Table III-3 provides an overview of the Pearson's coefficient of correlation for the most influential independent variables against the ASSTC for the 30 cm, 60 cm 90 cm, and 150 cm substrate depths. There was statistical significance in the correlations, which is an indication of a linear relationship between the independent variables and the ASSTC.

Table III-3: Pearson coefficient of correlation for independent variables against the ASSTC at various substrates for the winter.

	30 cm	60 cm	90 cm	150 cm
Pre-storm stage	-0.652	-0.709	-0.592	0.678
Peak-storm stage	-0.520	-0.616	-0.559	0.331
Amplitude of stream temperature change	0.511	0.468	0.496	0.085

However, the coefficients of correlations and the scatter plots (Figure III-4) indicate that there is a negative linearity between the independent variables; pre and peak-storm stage, whereas the amplitude of stream temperature change had a positive correlation with the ASSTC.

The pre-storm stage has an r = -0.652 for the shallow substrate (up to 30 cm) and an average r = -0.660 for the deeper substrate (60 cm to 150 cm). These r values result in a coefficient of determination $r^2 = 0.425$ for the shallow substrate and $r^2 = 0.436$ for the deeper substrate. The pre-storm stage accounts for 43% of variations in ASSTC which does not change between the upper and deeper substrates during the winter

Additionally, the peak-storm stage recorded an r = -0.520 for the shallow substrate, which diminishes to an average of r = -0.502 for the deeper substrate. This gives rise to

coefficient of determination $r^2 = 0.270$ for the shallow substrate and $r^2 = 0.252$ for the deeper substrate. During the winter, the peak-storm stage can explain 27.0% of the shallow ASSTC, which reduces to 25.2%.

Finally, the amplitude of stream temperature change correlated r = 0.511 for the shallow substrate, which mutes to an average r = 0.350 for the deeper substrate, which translate into a coefficient of determination $r^2 = 0.261$ for the shallow substrate and $r^2 = 0.123$ for the deeper substrate. The amplitude of stream temperature change is responsible 26.1% of the shallow ASSTC, whereas, it accounts for 12.3% of the observed after-storm temperature variations in the deeper substrate during the winter.

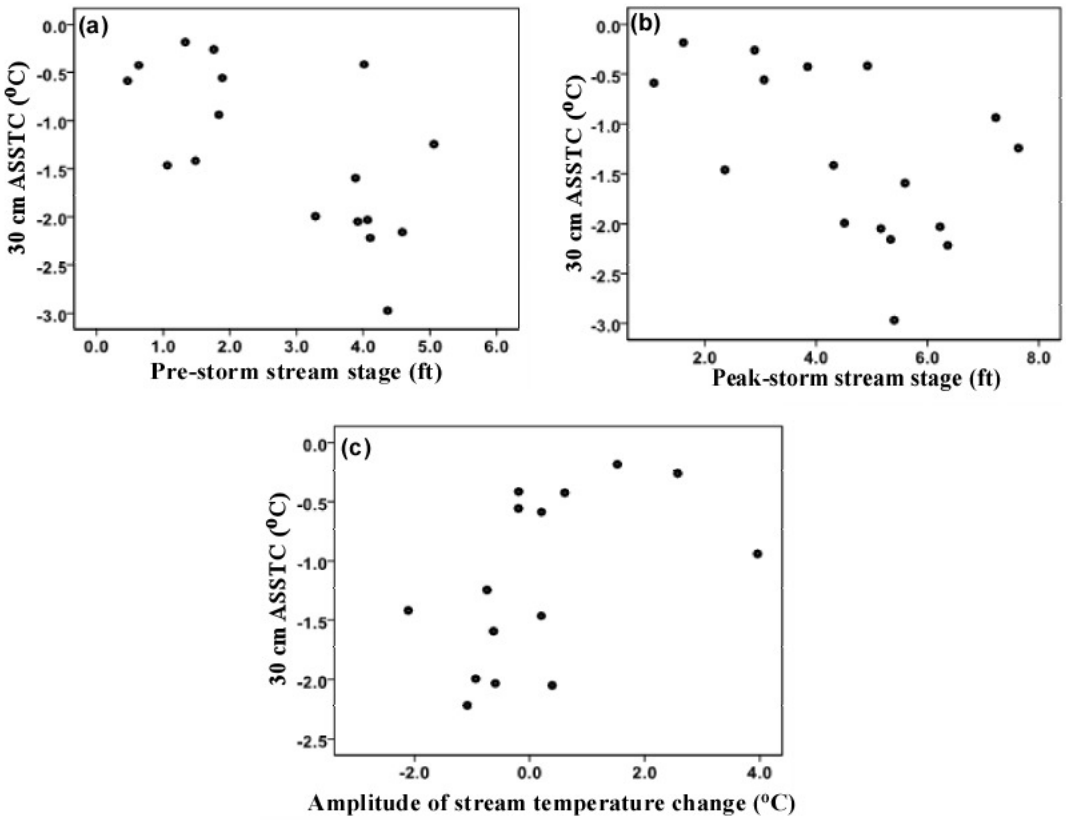

Figure III-4: Scatter plot of winter 30 cm ASSTC against a) pre-storm stream stage, b) peak-storm stream stage, c) amplitude of stream temperature change.

Summer

A summary of the Pearson's coefficient of correlation for the highest correlated independent variables against the after-storm temperature changes for the 30 cm, 60 cm 90 cm, and 150 cm substrate depths are provide in Table III-4. There is statistical significance in the correlations which is an indication of a linear relationship between the independent variables and the ASSTC.

Table III-4: Pearson coefficient of correlation for independent variables against the ASSTC at various substrates during summer.

	30 cm	60 cm	90 cm	150 cm
Amplitude of storm	0.490	0.521	0.552	0.638
Pre-storm stream temperature	0.379	0.356	0.293	0.301
Peak-storm stream temperature	0.468	0.400	0.308	0.345

The coefficients of correlation and the scatter plots (Figure III-5), however, indicate that there is positive linear correlation between the independent variables; amplitude of storm, pre-storm stream temperature and peak-storm stream temperature with the ASSTC.

The amplitude of the storm correlated r = 0.490 for the shallow substrate, whereas, it correlated an average r = 0.570 for the deeper substrate. This implies a coefficient of determination $r^2 = 0.240$ for the upper substrate and $r^2 = 0.325$ for the lower substrate. The amplitude of the storm is responsible for 24.0% of the observed ASSTC in the shallow substrate, which increases to 32.5% for the deeper substrate during the summer.

Furthermore, the pre-storm stream temperature has a correlation r = 0.379 for the shallow substrate, which mutes to an average r = 0.317 for the deeper substrate. This results in a coefficient of determination $r^2 = 0.144$ for the shallow substrate and $r^2 = 0.100$ for the deeper substrate. The pre-storm stream temperature can explain 14.4% of the

shallow ASSTC, whereas, it was responsible for 10.0% of the deeper ASSTC the summer.

Finally, the peak-storm stream temperature correlated r = 0.468 for the shallow substrate, whereas, it correlated an average r = 0.351 for the deeper substrate, which translates into a coefficient of determination $r^2 = 0.219$ for the upper substrate and $r^2 =$ 0.12.3 for the deeper substrate. The peak-storm stream temperature, therefore, is responsible for 21.9% of the observed variations in upper ASSTC and responsible for 12.3% of the deeper ASSTC during the summer.

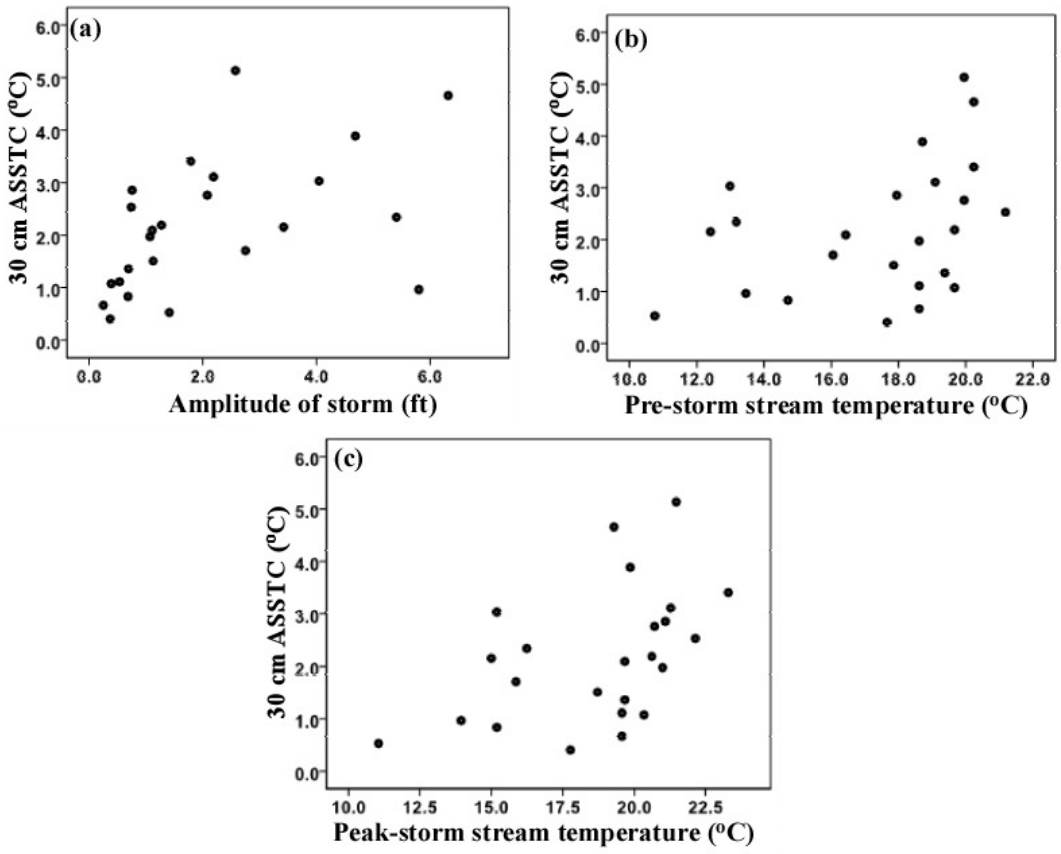

Figure III-5: Scatter plot of summer 30 cm ASSTC against a) amplitude of storm, b) pre-storm stream temperature, c) peak-storm stream temperature.

Combined Winter and Summer

Both the winter and summer data were combined to assess the overall relevant predictor variables for both seasons. Table III-5 summarizes the Pearson's coefficient of correlation for the overall predictor variables against the ASSTC for the 30 cm, 60 cm 90 cm, and 150 cm substrate depths. There is statistical significance in the correlations indicating a linear relationship between the independent variables and the ASSTC .

Table III-5: Pearson coefficient of correlation for independent variables against the ASSTC at various substrates for the entire year.

	30 cm	60 cm	90 cm	150 cm
Pre-storm stage	-0.614	-0.550	-0.448	-0.323
Amplitude of storm	0.265	0.340	0.380	0.323
Pre-storm stream temperature	0.826	0.768	0.702	0.671
Peak-storm stream temperature	0.855	0.787	0.713	0.680

The coefficients of correlation and the scatter plots (Figure III-6), however, indicate that there is positive linear correlation between the independent variables; amplitude of storm, pre and peak-storm stream temperature, whereas the pre-storm stage shows a negative correlation.

The pre-storm stage correlated r = -0.614 for the shallow substrate, whereas it correlated an average r = -0.440 for the deeper substrate. This implies a coefficient of determination $r^2 = 0.377$ for the upper substrate and $r^2 = 0.194$ for the lower substrate. The influence of pre-storm stage on ASSTC dampens from 37.7% for the upper substrate to 19.4% for the deeper substrate for the entire year.

Additionally, the amplitude of storm correlated r = 0.265 for the shallow substrate, whereas, it correlated an average r = 0.366 for the deeper substrate. This results in a coefficient of determination $r^2 = 0.07$ for the shallow substrate and $r^2 = 0.134$ for the

deeper substrate. The amplitude of storm shows a weak influence for the combined seasons, it controls 7.0% of the ASSTC in the upper substrate and 13.4% for the deeper substrate changes.

Finally, the pre and peak-storm stream temperatures show an equal correlations with average r = 0.841 for the shallow substrate, and average r = 0.720 for the deeper substrate. This translates into a coefficient of determination $r^2 = 0.707$ for the upper substrate and $r^2 = 0.493$ for the deeper substrate. The pre and peak-storm stream temperature have a strong influence for the combine seasons, accounting for 70.7% of the upper substrate changes, whereas it explains 49.3% of the deeper substrate responses.

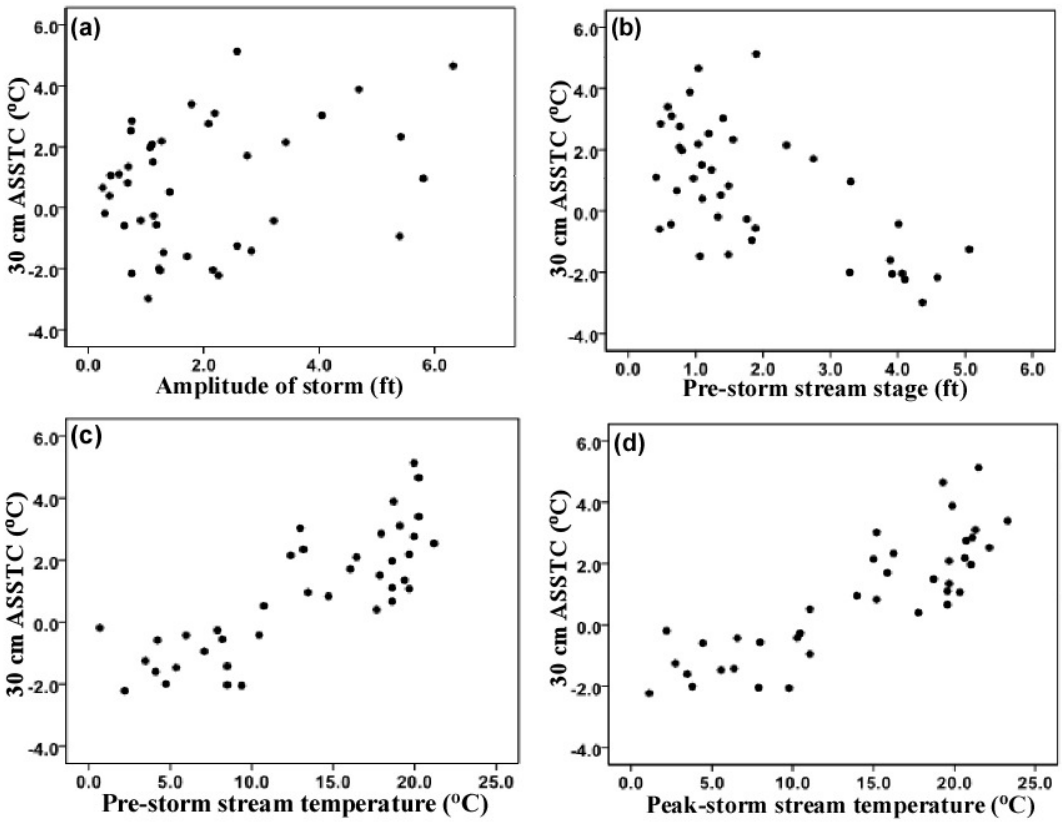

Figure III-6: Scatter plot of combined winter and summer 30 cm substrate temperature change against a) amplitude of storm, b) pre-storm stream stage, c) pre-storm stream temperature, d) peak-storm stream temperature.

Model Development

ASSTC Model

Analysis of the correlations of coefficient of the ASSTC against the various independent parameters indicate that the most relevant independent predictor variables for combined winter and summer seasons are the pre-storm stream stage, the amplitude of storm, the pre-storm stream temperature, and the peak-storm stream temperature. Using these independent predictor variables and the stepwise regression procedure (Mellina et al., 2002) the following ASSTC model was developed:

$$ASSTC = 10^{[0.313+0.018PSST+0.289Log_{10}(AS+2)]} - 5$$

Where AS = amplitude of storm, PSST = peak-storm stream temperature.

The adjusted R^2 (Table III-6) indicates that the model is able to predict ASSTC accurately 73.4% of the times.

Table III-6: Model summary

R	R^2	Adjusted R^2	Durbin-Watson	Max. Mahalanobis Distance	Max. Cook's Distance
0.861	0.740	0.734	2.516	5.188	0.127

Model Diagnostics

Regression diagnostics is used to explore the data to uncover anomalies such as multivariate outliers, the presence of autocorrelation, multicollinearity and to ensure that the assumptions underlying linear regression models are met.

The shape of the scatter plot of the transformed ASSTC against the unstandardized residual is fairly rectangular with minor fanning (Figure III-7a). Additionally, the residuals meet the normal theory assumption based on the distribution curve of the

regression standardized residual and the normal probability plot (Figure III-7c and 7d). These are indication that the assumptions underlying linear regression models are met (linearity, normality, and homoscedasticity). The regression standardized residuals against regression standardized predicted value plot (Figure III-7b), however, shows that there are two sets of residuals. The negative set representing the residuals of the winter prediction, whereas the positive set represents the residuals of the summer prediction. The residual distribution shows that the model's winter predictability is not as optimum as compared to its summer predictability.

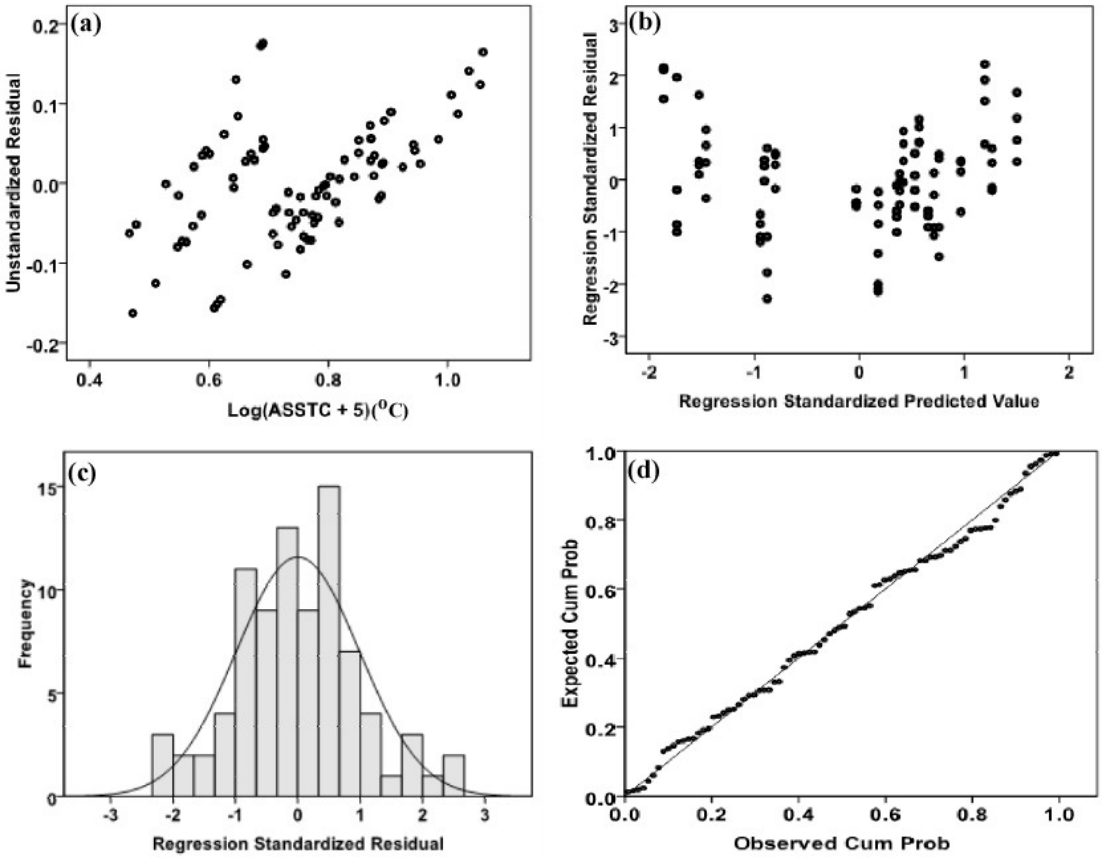

Figure III-7: scatter plot of a) transformed substrate temperature change against the unstandardized residuals b) regression standardized residuals against regression standardized predicted value, c) histogram of regression standardized residuals d) probability normality plot

The maximum Mahalanobis distance of 5.188 (Table III-6) is less than the critical value of 13.82 given the two independent variables in the ASSTC model. Additionally, the Cook's distance of 0.127 is significantly less than 1. These are indication of the absence of multivariate outliers in the data.

The Durbin-Watson statistic of 2.516 (Table III-6) which is not significantly greater than 2, is evidence of the absence of dependence or autocorrelation of errors.

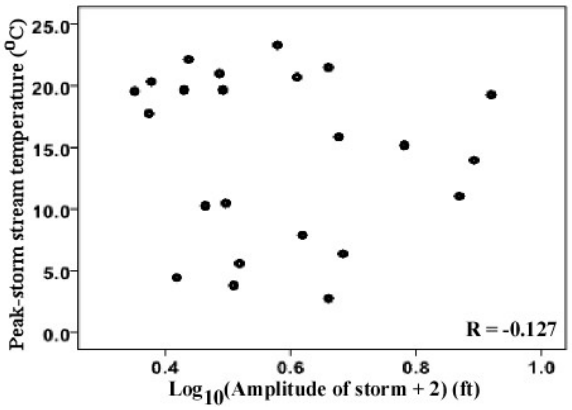

Figure III-8: scatter plot matrix and cross correlations of retained independent variables.

There is no statistical significance between the correlations of the retained independent variables, indicating the absence of a linear relationship (Figure III-8). The non-linear relationship is an indication of the absence of multicollinearity between the retained independent variables.

Model Verification

The model data fit and the model diagnostics show that a good model has been developed. The ability of the model, however, to predict new data is uncertain. We therefore validated the model using the model validation data, which were not used in fitting the model. This will help assess the ability of the model to predict future events.

The model verification showed an adjusted R^2 of 0.857 units which was better than the adjusted R^2 obtained during the model fitting. The plot of the observed ASSTC against simulated ASSTC (Figure III-9) and the adjusted R^2 show that the model is able to predict future events accurately 85.7% of the times between the temperature ranges of –2.5^{o}C to 4.0^{o}C. The near oval shape of the standardized residual plot (Figure III-10a), though not the best, shows that the assumption of linearity and uniformity of variance is met. Additionally, the residuals meet the normal theory assumption based on the shape of the normality plot of the standardized residuals and the normal probability plot though there is slit deviation from the line of best fit (Figure III-10b and 10c).

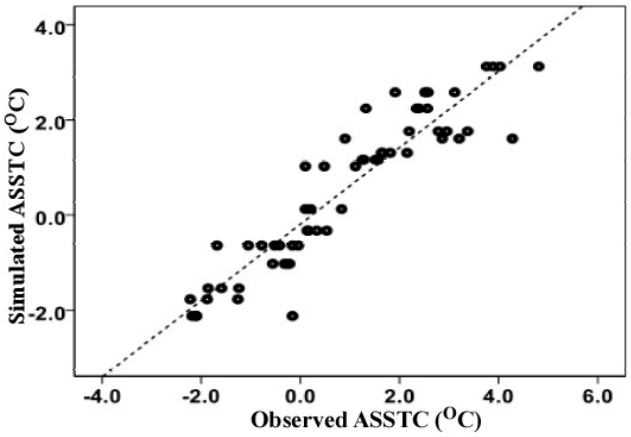

Figure III-9: a) scatter plot of simulated ASSTC against measured ASSTC

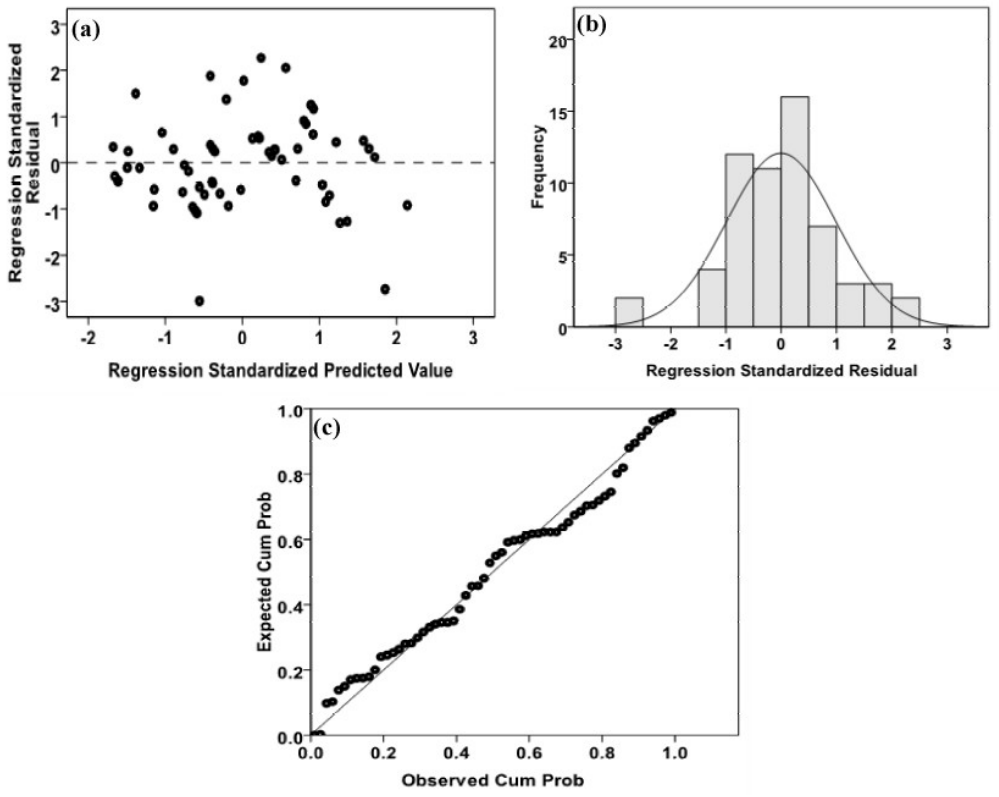

Figure III-10: a) scatter plot of the regression standardized predicted value against the regression standardized residuals, b) histogram of regression standardized residuals for the model verification.

Discussion

The predominant parameters controlling substrate temperature change during the winter season were the pre-storm and peak-storm stage, and the amplitude of stream temperature change (Table III-3). The amplitude of storm, the pre-storm and peak-storm stream temperatures, however, were the controlling parameters during the summer season (Table III-4). The combined seasons (entire year) had the pre-storm stage, the amplitude of storm, pre and peak-storm stream temperatures as the controlling predictor parameters.

During the winter, the pre-storm and peak-storm stage both had a negative linear relationship with the ASSTC. Pre and peak-storm stream temperature contributed an

average of 58.6% and 58.1% to the observed shallow and deeper ASSTCs respectively. The amplitude of stream temperature change, however, had a direct linear relationship with the ASSTC and contributed 51.1% and 35% to the upper and lower substrate responses respectively.

The pre-storm stage has more influence on substrate response compared to the amplitude of the storm during the winter season. The increased influence of the pre-storm stage, rather than the amplitude of the storm is because small pre-storm stage provides a thin shield for the shallow substrate. The thin shield over the streambed causes the hyporheic water to build a strong connection with the prevailing cold air temperature, creating a small thermal gradient between the temperature of the incoming runoff and the pre-storm substrate temperature. Therefore, an increase in the amplitude of storm will only inundate the substrate with a near thermally equilibrated water which will not have a lot of influence on the ASSTC. The small thermal gradient will result in a small ASSTC during mixing and thermal homogenization of the storm runoff and the pre-storm hyporheic water. As the substrate depth increases, however, the influence of the pre-storm stage diminishes, due to the buffering capacity provided by the upper substrate, which shields the deeper substrate from the prevailing air temperature (Evans and Peets, 1997). Additionally, during the winter, some of the high hydrologic flows were as a result of snow melt which has a different flow mechanics compared to storm runoff. This could also contribute to the less influence of the amplitude of the storm on ASSTC during the winter season.

When the pre-storm stage increases the stream water provides a thicker shield for the hyporheic water. The thicker shield prevents the hyporheic water from building a strong

connection with the prevailing air temperature. The substrate temperature, rather builds a strong connection with the warmer groundwater flux, which results in a steep thermal gradient between the colder incoming runoff and the warmer pre-storm substrate temperatures. The steep thermal gradient results in bigger ASSTC during the mixing and thermal homogenization of the colder storm runoff and warmer pre-storm hyporheic water.

ASSTC increased with increase in amplitude of stream temperature change, which is due to the strong connection between the stream temperature and the upper substrate temperatures (Dogwiler and Wicks, 2006). The influence of the amplitude of stream temperature change dampened with increasing depth because the connection between the stream temperature and the substrate diminishes with increasing substrate depth, because the sedimentological composition of the streambed acts as a "mechanical filter" to the surface thermal inputs (Vervier *et al*., 1992).

During the summer, however, the amplitude of the storm had a positive linear relationship with the ASSTC and contributed 49% and 57% to the observed shallow and deeper ASSTCs respectively. The pre and peak-storm stream temperatures, similarly, each had a direct linear relationship with the ASSTC and contributed an average of 42.4% and 33.4% to the upper and deeper substrate responses respectively.

The amplitude of the storm rather than the pre-storm stage controlled the after-storm substrate response during the summer. There are frequent fluctuations in the pre-storm stage during the summer due to diurnal heating (Casie, 2006) and evaporation of the stream water. Therefore, the pre-storm stage, irrespective of the height is unable to provide so much protection for the streambed, which results in the pre-storm stage not to

have much influence on the summer ASSTC. There was a steep thermal gradient between the pre-storm stream temperature and the pre-storm substrate temperatures during the summer. The steep thermal gradient means a bigger amplitude storm will inundate the substrate with a lot of thermally unequilibrated stream water, which will result in a bigger substrate response during mixing and thermal homogenization of the stream water with the hyporheic water. A smaller amplitude storm, however, will have a reduced influence on the ASSTC because there will not be a lot of thermally unequilibrated stream water to inundate the substrate with, which will lead to a smaller substrate response during mixing and thermal homogenization. There is, therefore, a direct relationship between the amplitude of the storm and the amplitude of after-storm substrate thermal response during the summer.

The influence of the amplitude of the storm increased with increasing depth. Bigger storm amplitudes are able to push more water deeper into the substrate, whereas both smaller and bigger storm amplitudes will still get water into the shallow substrate. The amplitude of the storm, therefore, becomes more important to the deeper substrate resulting in an increased influence of the amplitude of the storm with increasing depth. Additionally, increase storm amplitude coupled with the light density of warm water increases the seepage rate during the summer. The work of Constantz (1998) showed an increase in seepage rate with increasing temperature due to changes in water density and dynamic viscosity. Thus, the influence of the amplitude of the storm is able to penetrate deeper into the streambed during the summer.

The entire year's data show that the pre-storm stage, the amplitude of the storm, pre and peak-storm stream temperatures are the controlling variables for the ASSTC, which

is a combination of the winter and summer controlling variables. The proposed ASSTC model based on the amplitude of storm and the peak-storm stream temperature appears to predict the ASSTC for the entire year. The slope of the amplitude of the storm in the ASSTC model indicates a strong influence of the amplitude of storm on ASSTC, which is consistent with the observation made by Dogwiler and Wicks (2006), and Brown and Hannah (2007). Dogwiller and Wicks (2006) indicated that the after storm stream temperature changes depend on the temperature of the incoming storm runoff and the temperature of the frontal passage. The peak-storm stream temperature, which is the second independent variable, therefore depends on the temperature of the incoming runoff and the frontal passage. The model therefore indicates that the influences of the temperature of the incoming runoff and the frontal passage are transmitted into the substrate after a storm.

The adjusted coefficient of determination of 0.734 units for the ASSTC predictive model indicates that the model fits the data well. The low adjusted R^2, however, is due to the prevalence of geologic heterogeneity in the streambed which can cause significantly different thermal patterns (Ringler and Hall, 1975; Evans *et al*., 1995), and also the variance between the winter and summer conditions, which makes it difficult to fit a model for both seasons. The ASSTC model, however, did a better job in the model verification with an increased adjusted R^2 of 0.858 units for the model verification. The increased adjusted R^2 shows a good ability of the model to predict future events, and therefore provides a tool for predicting ASSTC. The user however, should be weary of the model's less accuracy in predicting winter ASSTC. All the residual plots and the model diagnostic procedures indicate that the model meets all the assumptions of linear

regression and can solely be used to predict ASSTC. The ASSTC model, however, is intended for use for substrate depths of 30 cm to 150 cm and for a third-order sand and gravel bedded stream. The accuracy outside of these conditions is unknown.

Conclusion

The focus of this study was to assess the relevant predictor variables of ASSTC and to fit a predictive model in estimating future ASSTCs. The results of the study show that different independent variables control each season. Pre and peak-storm stage and amplitude of stream temperature change control winter ASSTC, whereas, the amplitude of storm and the pre and peak-storm stream temperatures are the relevant independent predictor parameters of summer ASSTC. Analysis of the combined season's data revealed that the pre-storm stage, the amplitude of the storm, the pre and peak-storm stream temperatures control the entire year's ASSTC.

The results indicate that a simple curvilinear regression model based on the amplitude of storm and the peak-storm stream temperature could be used to predict ASSTC for the entire year. The performance of the ASSTC model during the winter season, however, is not optimum and also the simulation of the model is more reliable between ASSTC of -2.5^{o}C to 4^{o}C. Nevertheless, this model will aid resource managers in the investigation and management of aquatic ecosystem within the hyporheic zone after a storm event, given the importance of the impact of acute temperature changes on aquatic stability

References

Brown LE & Hannah DM (2007) Alpine stream temperature response to storm events. *Journal of Hydrometeorology* **8**: 952-967.

Casie D (2006) The thermal regime of rivers: A review. Freshwater Biol., **51**: 1389-1406.

Conant B Jr. (2004) Delineating and Quantifying Ground Water Discharge Zones Using Streambed Temperatures. *Ground Water* **42**: 243-257.

Constantz J (1998) Interaction between stream temperature, streamflow and groundwater exchanges in alpine streams. *Water Resour. Res*. **34**: 1609-1616.

Dogwiler T & Wicks C (2006) Thermal variation in the hyporheic zone of a karst stream. *International journal of Speleology* **35**: 59-66.

Evans EC & Petts GE (1997) Hyporheic temperature patterns within riffles. Hydrological Sciences Journal **42**: 199-213.

Evans EC, Greenwood MT & Petts GE (1995) Short communication: Thermal profiles within river beds. *Hydrol. Processes.* **9**: 19-25.

Galloway BJ & Kieffer JD (2003) The Effects of an Acute Temperature Change on the Metabolic Recovery from Exhaustive Exercise in Juvenile Atlantic Salmon (Salmo salar). *Physiological and Biochemical Zoology* **76(5)**: 652–662.

Gilbert J, Dole-Olivier MJ, Marmonier P & Vervier P (1990) Surface water/ groundwater ecotones. *In: Ecology and Management of Aquatic Terrestial Ecotones. Man and Biosphere.* Ed. By R. J. Naiman & H. Decamps, 199-225. UNESCO, Paris & Parthenon Publishers, Carnforth, UK.

Hannah DM, Malcom IA, Soulsby C & Youngson AF (2004) Heat exchanges and temperatures within a salmon spawning stream in the Cairngorms, Scotland: Seasonal and subseasonal dynamics. *Riv. Res. Apps*. **20**: 635-652.

Hayashi M, Rosenberry DO (2002) Effects of ground water exchange on the hydrology and ecology of surface water. *Ground Water* **40**: 309-316.

Hynes HBN (1970) *The Ecology of Running Waters.* Liverpool University Press, Liverpool, UK.

Hynes HBN (1983) Groundwater and stream ecology. *Hydrobiologia* **100**: 93-99.

Hynes HBN, Williams DD & Williams NE (1976) Distribution of the benthos within the substratum of a Welsh mountain stream. *Oikos* **27**: 307-310.

Kabayashi D, Ishii Y, & Kodama Y (1999) Stream temperature, specific conductance and runoff process in mountain watersheds. *Hydrological Processes*, **13**: 865-876.

Mellina E, Moore RD, Hinch SG, Macdonald JS & Pearson G (2002) Stream temperature response to clearcut logging in British Columbia: the moderating influences of groundwater and headwater lakes. *Can. J. Fish. Aquat. Sci*. **59**: 1886-1900

Mitchell S (1999) A simple Model for Estimating Mean Monthly Stream Temperatures After Riparian Canopy Removal. Environmental Management, **24**: No. 1, pp. 77-83

Neumann DW, Rajagopalan B & Zagona EA (2003) Regression Model for Daily Maximum Stream Temperature. *Journal of Environmental Engineering*, **129**: No. 7 (667)

Peterson EW & Sickbert TB (2006) Stream water bypass through a meander neck, laterally extending the hyporheic zone. *Hydrogeology Journal* **14**: 1443-1451. DOI: 10.1007/s10040-006-0050-3.

Poole WL & Stewart KW (1976) The vertical distribution of macrobenthos within the substratum of the Brazos River, Texas. *Hydrobiolobia* **50**: 151-160.

Ringler NH & Hall JD (1975) Effects of logging on water temperature and dissolved oxygen in spawning beds. *Trans. Am. Fish. Soc*. **104**: 111-121.

Shepherd BG (1984) Predicted impacts of altered water temperature regime on Glendale Creek pink fry. *Canadian MS Report on Fisheries and Aquatic Science,* no. 1782

Stanford JA & Ward JV (1988) The hyporheic habitat of river ecosystem: *Nature*, **335**: 64–66.

Tabachnick BG & Fidell LS (1989) *Using multivariate statistics*. Harper Collins Publishers, Second Edition.

Vannote RL & Sweeney BW (1980) Geographic analysis of thermal equllibria: a

conceptual model for evaluating the effect of natural and modified thermal regimes on aquatic insect communities. *American Naturalist,* **115**: 667-695.

Vervier P, Gilbert J, Dole-Olivier MJ & Marmonier P (1992) A perspective on the permeability on the surface freshwater-groundwater ecotone, *J. North Am. Benthol. Soc.* **11**: 93-102.

Ward JV (1989) The four-dimensional nature of lotic ecosystems. *Journal of the North American Benthological Society*, **8**: 2-8.

Wickett WP (1954) The oxygen supply to salmon eggs in spawning beds. *J. Fish. Res. Bd. Can*. **11**: 933-953.

CHAPTER IV

SUMMARY OF CONCLUSIONS

There was clear seasonal differences in the ASSTC with winter substrates responding to the storm event with drops, whereas, the summer substrate responded with spikes, which implies a seasonal thermal reverse in after-storm substrate response. The depth of wetting front of a storm event determines the depth to which advective transport controls thermal transmission into the substrate. The acute temperature change at the depth of the wetting front creates a steep thermal gradient, which induces conductive transport that further propagates heat into the deeper substrate. Nonetheless, advection dominates ($P_e = 34.1$) the overall vertical heat transport after a storm event. In addition to advection and conduction controlling vertical temperature transmission into the substrate, the amplitude of the vertical responses dampens with increasing depth. There are however, no significant differences in the dampening responses with increasing depth in the summer, whereas, the winter response showed significant difference at 150 cm depth at 0.05 level of significance.

Pre-storm stage (antecedent basin conditions) and amplitude of stream temperature change are the most relevant controlling parameters on the ASSTC during the winter, whereas, the amplitude of storm and the pre-storm stream temperature were the relevant independent predictor parameters of ASSTC during the summer, which implies different controlling parameters for the two seasons. The entire year's ASSTC, however, is controlled by the pre-storm stage, amplitude of storm and pre and peak-storm stream temperatures. A simple curvilinear regression model based on the amplitude of storm and the peak-storm stream temperature was fitted to predict summer ASSTC. The most relevant predictors based on the ASSTC model are therefore, the amplitude of storm and the peak-storm stream temperature.

REFERENCES

Anderson MP (2005) Heat as a groundwater tracer. *Ground water* **43: no. 6:** 951-968

Atwell BH, MacDonald RB, & Bartolucci LA (1971) Thermal mapping of streams from airborne radiometric scanning. *Water Res. Bull.,* **7(2)**: 228-243.

Bencala KE (2000) Hyporheic zone hydrological processes. *Hydrological Processes* **14, no. 15**: 2797–2798.

Boulton AJ, Findlay S, Marmonier P, Stanley EH and Valett HM (1998) The functional significance of the Hyporheic zone in streams and rivers. *Annual Review of Ecology and Systematics* **29**: 59–81.

Brown LE & Hannah DM (2007) Alpine stream temperature response to storm events. *Journal of Hydrometeorology* **8**: 952-967.

Cartwright K, Hunt CS, Hughes G. and Brower RD (1979) Hydraulic potential in Lake Michigan bottom sediments. *J. Hydrol*., **43**: 67-78.

Constantz J, Cox MH & Su GW (2003) Comparison of heat and bromide as ground water tracers near streams. *Ground Water* **41**: 647-656.

Hayashi M, Rosenberry DO (2002) Effects of ground water exchange on the hydrology and ecology of surface water. *Ground Water* **40**: 309-316.

Kabayashi D, Ishii Y, & Kodama Y (1999) Stream temperature, specific conductance and runoff process in mountain watersheds. *Hydrological Processes*, **13**: 865-876.

Kenoyer GJ and Anderson MP (1989) Groundwater's dynamic role in regulating acidity and chemistry in a precipitation-dominated lake. *J. Hydrol*., **109**: 287-306.

Lee DR (1977) A device for measuring seepage flux in lakes and estuaries. *Limnol. Oceanogr*., **22(1)**: 140- 147.

Lee DR (1985) Method for locating sediment anomalies in lake beds that can be caused by groundwater inflow. *J. Hydrol*., **79**:187 193.

Nelson J (1991) Analysis of thermal scanning imagery and physical sampling to investigate point inflows to surface water bodies. *Mater's Thesis, University of Notre Dame*, 121 pp.

Silliman SE & Booth DF (1993) Analysis of time-series measurements of sediment temperature for identification of gaining vs. losing portions of Juday Creek, Indiana. *Journal of Hydrogeology* **146**: 131-148.

Souto-Maior J (1973) Applications of thermal remote sensing to detailed groundwater studies. Remote Sensing and Water Resources Management, *Am Water Res. Assoc*. Bethesda, MD, pp. 284-299.

Stonestrom DA and Constantz J (2004) Heat as a tool for studying the movement of ground water near streams. *USGS Circular 1260*. Reston, Virginia: USGS.

Winter TC (1978a) Numerical simulation of steady-state three-dimensional groundwater flow through lakes. *Water Resource. Res*., **14(2)**: 245-254.

Winter TC (1978b) Groundwater component of lake water and nutrient budgets. Verb. Int. Ver. Limno, **20**: 438-444

Winter TC (1981) Uncertainties in estimating the water balances of lakes. Water Res. Bull. **17**: 85-115.

Winter TC (1983) The interaction of lakes with variably saturated porous media. Water Res. Res. **19(5)**: 1203-1218.

Winter TC (1986) Effect of groundwater recharge on configuration of the water table beneath sand dunes and on seepage lakes in the sandhills of Nebraska, USA. *J. Hydrol*., **86**: 221-237.